Accepted Manuscript

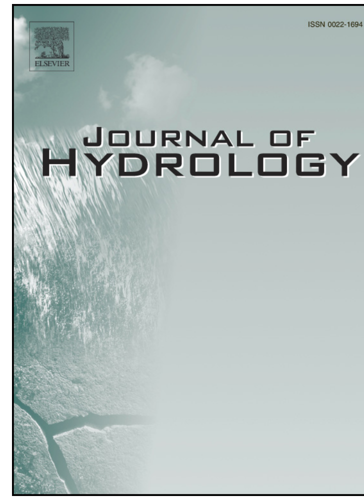

Determination of vertical hydraulic conductivity of aquitards in a multilayered leaky system using water-level signals in adjacent aquifers

Zhenjiao Jiang, Gregoire Mariethoz, Mauricio Taulis, Malcolm Cox

PII: S0022-1694(13)00557-X
DOI: http://dx.doi.org/10.1016/j.jhydrol.2013.07.030
Reference: HYDROL 19017

To appear in: *Journal of Hydrology*

Received Date: 19 April 2013
Revised Date: 1 July 2013
Accepted Date: 22 July 2013

Please cite this article as: Jiang, Z., Mariethoz, G., Taulis, M., Cox, M., Determination of vertical hydraulic conductivity of aquitards in a multilayered leaky system using water-level signals in adjacent aquifers, *Journal of Hydrology* (2013), doi: http://dx.doi.org/10.1016/j.jhydrol.2013.07.030

Determination of vertical hydraulic conductivity of aquitards in a multilayered leaky system using water-level signals in adjacent aquifers

Zhenjiao Jiang [a,*], Gregoire Mariethoz [b], Mauricio Taulis [a], Malcolm Cox [a]

[a] School of Earth, Environmental & Biological Sciences, Queensland University of Technology, GP campus, 4001, Brisbane, Australia.

[b] School of Civil and Environmental Engineering, University of New South Wales, UNSW 2052, Sydney, Australia

Zhenjiao Jiang (corresponding author)

Email: z1.jiang@qut.edu.au

Abstract

This paper presents a methodology for determining the vertical hydraulic conductivity (K_v) of an aquitard, in a multilayered leaky system, based on the harmonic analysis of arbitrary water-level fluctuations in aquifers. As a result, K_v of the aquitard is expressed as a function of the phase-shift of water-level signals measured in the two adjacent aquifers. Based on this expression, we propose a robust method to calculate K_v by employing linear regression analysis of logarithm transformed frequencies and phases. The frequencies, where the K_v is calculated, are identified by coherence analysis. The proposed methods are validated by a synthetic case study and are then applied to the Westbourne and Birkhead aquitards, which form part of a five-layered leaky system in the Eromanga Basin, Australia.

Keywords

Hydraulic conductivity; aquitard; harmonic analysis approach; coherence; Great Artesian Basin.

1.Introduction

Determination of the vertical hydraulic conductivity (K_v) of aquitards is an important task for understanding hydraulic connection of an aquifer-aquitard systems (Eaton and Bradbury, 2003) and protecting groundwater from contamination (Hart et al., 2005; Remenda and van der Kamp, 1997). The K_v of an aquitard can be measured with laboratory tests (e.g. Arns et al., 2001; Timms and Hendry, 2008). However, these results may be several orders of magnitude different to the K_v required in the real-world study, because aquitards are generally heterogeneous and rock structures are disrupted during the sampling (Clauser, 1992; Schulze-Makuch et al., 1999). In contrast, *in situ* approaches are generally preferred as they can yield directly field-related values.

Commonly used *in situ* methods include pumping tests and slug tests (van der Kamp, 2001). During these tests, drawdowns are measured and plotted against elapsed time to produce an experimental curve. Hydraulic parameters of the aquifer and aquitard can be estimated by matching the experimental curve with a theoretical model. The theory supporting the analysis of K_v of the aquitard in a leaky aquifer system was developed by Hantush and Jacob (1955) and Hantush (1960). Neuman and Witherspoon (1969a; 1969b) improved the Hantush-Jacob solution by considering the storage ability of the aquitard and water-level responses in the unpumped aquifer. However, in a two-aquifer-one-aquitard leaky system, the drawdown in each aquifer depends on five dimensionless hydraulic parameters. In order to establish theoretical curves to cover the entire range of values necessary for the analysis of K_v, the ratio method is used (Neuman and Witherspoon, 1972; Wolff, 1970).

The ratio method, however, required drawdowns either increase or decrease regularly relating to the determined extraction/injection stresses. The current interest is to estimate the K_v of an aquitard based on arbitrary water-level fluctuations, which are caused by multiple underdetermined stresses. The deconvolution method was applied to such situation because water-level fluctuations induced by leakage via the aquitard follow the convolution relation (Neuman and Witherspoon, 1968):

$$s_2(t) = h(t) \otimes s_1(t) = \int_0^t s_1(\tau)h(t-\tau)d\tau \, , \tag{1}$$

where $s_1(t)$ and $s_2(t)$ represent water-level fluctuations measured at different depths in one aquitard, and $h(t)$ is a loss function expressed by means of Duhamel's function (Neuman and Gardner, 1989; Neuman and Witherspoon, 1968).

The deconvolution approach proposed by Neuman and Gardner (1989) was carried out by minimizing differences between measured and theoretical drawdown. Those differences were a function of hydraulic diffusivity and background water-level fluctuations in the aquifer.

An alternative deconvolution method is based on the Fourier transform, and referred to as harmonic analysis method (Boldt-Leppin and Hendry, 2003). In this method, water-level fluctuations, measured at different depths in the aquitard, are decomposed into a sum of trigonometric components of different frequencies. These trigonometric components are defined as harmonic signals. The hydraulic diffusivity is expressed analytically either based on the amplitude or phase shift of harmonic signals. However, the harmonic analysis approach, by now, assumes that the thickness of the aquitard is half infinite, which limits its application.

In this study, we apply the harmonic analysis method in a multilayered leaky system where the thickness of the aquitard is finite and both the top and bottom of the aquitard is bounded by aquifers. The aim is to calculate K_v of the aquitard based on a pair of water-level signals measured in the two adjacent aquifers. The water-level fluctuations in the aquifers may be induced by many factors (e.g. pumping, recharge, leakage or earthquake). However, only leakage-induced water-level fluctuations can represent the properties of the aquitard and so can be used to infer the K_v of the aquitard. Therefore, it is desirable to find a method to identify the leakage-induced water-level fluctuations in the aquifers. Coherence analysis is proposed for this purpose.

Coherence was originally defined and used in signal processing, which analyses the cross correlation between two signals in the frequency domain (Carter, 1987). It was used in hydrogeology to understand the hydraulic connection in karstic aquifer systems (Larocque et al., 1998; Padilla and Pulido-Bosch, 1995). The coherence varies from 0 to 1.0 depending on the degree to which the convolution relationship in Eq. (1) is satisfied. In this study, its value is determined by the degree to which leakage-induced water-level signals are interrupted by other factors. A weak interruption corresponds to a large coherence value.

In this study, we first derive analytical expression for K_v by using the harmonic analysis method in the three-layered leaky system. Following this, the method to calculate phases and the definition of coherence are introduced briefly and a robust method to estimate K_v is proposed. As support, the methods are validated in a simulated case and are applied to the eastern Eromanga Basin, Queensland, Australia.

2. Methods

2.1 Harmonic analysis of water-level signals

The harmonic analysis method was used to analyse K_v in aquitards of infinite thickness (Boldt-Leppin and Hendry, 2003), and here is applied to a three-layered leaky system, where the aquitard is bounded by two aquifers (Fig. 1a). The derivation is based on an analysis of water-level signal processes in the aquifers and aquitard, with the following assumptions:

(1) aquifers and aquitards have a homogeneous hydraulic conductivity;

(2) groundwater flow direction is vertical in the aquitard. This assumption is realistic when the permeability- contrast between the aquifer and aquitard exceeds a factor of 100 (Neuman and Witherspoon, 1969a);

(3) water-level changes in one aquifer cause detectable responses in its adjacent aquifer due to the leakage via the aquitard. In other words, there is a causal relationship for groundwater-level variations at different aquifers due to the leakage;

(4) water-level changes induced by the leakage at a small element are considered to propagate half-spherically in the aquifer (Fig. 1b-3), and we assume that the top of the upper aquifer and the bottom of the lower aquifer do not affect the propagation significantly;

(5) water levels propagate in the aquifers instantaneously, and time lags between stresses and observation wells in the aquifer are ignored.

Assumptions (1) - (2) are widely used in the analytical estimates of K_v by *in situ* methods. The discussions about their effects can be found in Neuman and Witherspoon (1969a; 1969b). The effects of assumptions (3) - (5) will be examined in the synthetic case study of section 3.1.

Derivation of K_v starts by adding an arbitrary water-level signal (s_0) at the top of the aquitard within a small area of dA (Fig. 1b-1 and 1c). The vertical transport of signal s_0 in the aquitard is described mathematically as:

$$\frac{\partial^2 s}{\partial z^2} = \frac{1}{\eta}\frac{\partial s}{\partial t}, \tag{2}$$

where η is the vertical hydraulic diffusivity of the aquitard which is defined as $\eta = K_v / S_s$ (m^2/d), K_v is the vertical hydraulic conductivity in the aquitard (m/d) and S_s is the specific storage (m^{-1}).

Before the signal reaches the lower aquifer (Fig. 1b-2), the aquitard behaves as if infinitely thick (Herrera and Figueroa V, 1969; Neuman and Witherspoon, 1972). At this stage, the water levels in the aquitard can be written in the frequency domain as:

$$s(f,\phi,z) = s_0(f,\phi)e^{(-Dz)}, \tag{3}$$

where $D = \sqrt{\frac{\pi f}{\eta}}(1+i)$, $i = \sqrt{-1}$, f is the frequency, ϕ is the phase, z is the depth in the aquitard, z=0 and z=b at the top and bottom of the aquitard, respectively, and b is thickness of the aquitard. Hereafter, the term $s(f, \phi, z)$ is denoted as s for convenience.

Since the aquitard is bounded by both aquifers, the signal expressed in Eq. (3) can reach the aquifer and induce the water-level changes in the aquifer; inversely, the situation in the aquifer will also affect the water-level signal in the aquitard. The aim of this study is to calculate the K_v using leakage-induced water-level changes in the aquifers. This requires that effective energy of water-level signal can penetrate the aquitard. Eq. (3) indicates that the energy of the signal occurring on the top of the aquitard (s_0) decays by a coefficient of $e^{-\sqrt{\frac{\pi f}{\eta}}z}$. We define an energy effectiveness (E), and that the decay coefficient satisfies $e^{-\sqrt{\frac{\pi f}{\eta}}b} \geq E$. This leads to the definition of a maximum frequency that allows the calculation of K_v:

$$f_{\max} = \frac{\imath d}{b^2}, \tag{4}$$

where d is the characteristic coefficient which can be expressed as: $d = \frac{[\ln(E)]^2}{\pi}$. The selection of both E and d will be discussed in section 3.1.3.

Once the signal s reaches the lower aquifer, water-level changes are induced by the leakage and propagate instantaneously in this aquifer (Dagan, 1989). The propagation of water levels in a half spherical space (Fig. 1b-3) can be described by:

$$Q^{-} = -2\pi r^{2} K^{-} \frac{ds_1^{-}}{dr}, \tag{5}$$

where the subscript '-' represents the quantities in the lower aquifer (and hereafter subscript '+' represents the upper aquifer), Q is the flow rate induced by the leakage through the aquitard, r is the distance between observation well and source/sink point (Fig. 1c), K is the radial hydraulic conductivity and s_1 is the water-level changes in the observation well induced by leakage through an area of dA, which can be given as:

$$dA = r_o dr_o d\theta, \tag{6}$$

where r_o and θ are the polar coordinates centred by the observation well (Fig. 1c).

The leakage from the aquitard at dA is considered as a point source or sink for the aquifers, the flow rate of which is described by Darcy's Law:

$$Q^{-} = -K_v \frac{ds}{dz} \cdot dA. \tag{7}$$

Making use of Eq. (3) in (7), at the bottom of the aquitard, yields,

$$Q^{-} = K_v D e^{-Db} s_0 \cdot dA. \tag{8}$$

Equating Eqs. (5) and (8) leads to,

$$s_1^{-}(r^{-}, f) = \int_{r^{-}}^{R'} \frac{K_v D e^{-Db} s_0 \cdot dA}{2\pi K^{-}} \frac{1}{r^{2}} dr, \tag{9}$$

where R' is the influence radius of the leakage occurring at dA, and $s_1^{-}(R', f) = 0$. In general, $R' >> r^{-}$. Note that r in Eq. (9) is centred at dA, which is different with the coordinate system in Eq. (6) where r_o is centred at the observation well. Hence, dA in this integral (Eq. 9) is treated as constant. Consequently, we obtain:

$$s_1^{-} = \frac{1}{r^{-}} \frac{K_v D}{2\pi K^{-}} s_0 e^{-Db} \cdot dA = \frac{1}{r^{-}} \xi_1 s_0 e^{-Db} \cdot dA. \tag{10}$$

Eq. (10) represents the water-level responses to signal s_0 in the lower aquifer induced by the leakage through the aquitard. Similarly, we can also write the water-level changes induced by the leakage in the upper aquifer as:

$$s_1^+ = -\frac{1}{r^+}\frac{K_v D}{2\pi K^+} s_0 dA = -\frac{1}{r^+}\xi_2 s_0 dA, \tag{11}$$

where $\xi_1 = \dfrac{K_v D}{2\pi K^-}$ and $\xi_2 = \dfrac{K_v D}{2\pi K^+}$.

Eqs. (10) and (11) express the first responses of aquifers to the initial signal s_0. According to the continuity condition, both water level and flux at the interface between aquitard and aquifer need to be balanced. In the above derivation, the flux balance is satisfied by equating Eqs. (5) and (8). However, water-level balance may not be satisfied after only one response to initial signal s_0. In this case, due to the instability on the interface, the water-level changes in the aquifer feedback on the aquitard and transport via the aquitard to affect opposite aquifers, and induce the second water-level responses in both aquifers. Subsequently, water levels in lower and upper aquifers are revised as:

$$s_2^- = \frac{1}{r^-}\xi_1(1-\xi_2)e^{-Db} s_0 dA, \tag{12}$$

and

$$s_2^+ = -\frac{1}{r^+}\xi_2(1-\xi_1 e^{-2Db}) s_0 dA. \tag{13}$$

This iterative process is repeated n times until the water-level balance is satisfied on the aquifer-aquitard interfaces. Because the propagation velocity of the pressure wave is infinitely large, the iteration processes is achieved instantly (Detournay, 1993). After nth iteration, the water-level fluctuation, induced by the leakage, in both aquifers can be expressed as:

$$s_n^- = \xi_1 s_0 e^{(-Db)} \mathbf{W}^- \mathbf{U} \frac{1}{r^-} dA, \tag{14}$$

$$s_n^+ = -\xi_2 s_0 \mathbf{W}^+ \mathbf{U} \frac{1}{r^+} dA \,, \tag{15}$$

where, $\mathbf{W}^- = [1, \xi_2, \xi_1\xi_2 e^{-2Db}, \xi_1\xi_2^2 e^{-2Db}, ..., \xi_1^{floor(\frac{n-1}{2})} \xi_2^{floor(\frac{n}{2})} e^{-2\,floor(\frac{n-1}{2})Db}]$,

$\mathbf{W}^+ = [1, \xi_1 e^{-2Db}, \xi_1\xi_2 e^{-2Db}, ...,. \xi_1^{floor(\frac{n}{2})} \xi_2^{floor(\frac{n-1}{2})} e^{-2\,floor(\frac{n}{2})Db}]$,

$\mathbf{U} = \left[1, (-1)(n-1), \binom{n-1}{2}, ...(-1)^{n-1}\binom{n-1}{n-1}\right]^T$, $n \geq 1$ and $\binom{n-1}{m} = \dfrac{(n-1)(n-2)...(n-m)}{m!}$,

$_T$ is the transpose operator and *floor*() rounds the value to the smaller nearest integer.

Eqs. (14) and (15) are the general solution for leakage-induced water-level fluctuations in the lower and upper aquifer, respectively. If water level at the interface reaches the balance after the first response, no feedback processes occur. Therefore, at n=1, Eqs. (14) and (15) is the same as Eqs. (10) and (11), respectively.

Defining that:

$$\lambda_1 = \sum_{m=0}^{floor(\frac{n-1}{2})} \binom{n-1}{2m} (\xi_1\xi_2 e^{-2Db})^m \,,$$
$$\lambda_2 = \sum_{m=0}^{floor(\frac{n-2}{2})} \binom{n-1}{2m+1} (\xi_1\xi_2 e^{-2Db})^m \,, \tag{16}$$

the terms of $\mathbf{WU}$ in Eqs. (14) and (15) can be rewritten as:

$$\mathbf{W}^-\mathbf{U} = \lambda_1 + \xi_2\lambda_2 \,,$$
$$\mathbf{W}^+\mathbf{U} = \lambda_1 + \xi_1 e^{-2Db}\lambda_2 \,. \tag{17}$$

For the aquitard, both ξ_2 and ξ_1 are far less than 1.0. Due to this, first, both λ_1 and λ_2 can converge to zero under a small n and then the water-level balance on the interfaces are reached; second,

$$\mathbf{W}^{-}\mathbf{U} \approx \mathbf{W}^{+}\mathbf{U} = \lambda_1 . \tag{18}$$

Eqs. (14) and (15) express water-level fluctuations in each aquifer induced by an original stress s_0 at the small area of dA. A typically real case with respect to this result is that the water-level changes in both aquifers are induced by a single pumping well in one aquifer. More generally, the arbitrary water-level fluctuations in one aquifer can be induced by multiple point stresses or planar stresses. Define that,

$$\begin{aligned} &s_0(r,\theta,f) = 0 \text{ at the locations without original stresses,} \\ &s_0(r,\theta,f) \neq 0 \text{ at the locations that original stresses occurs.} \end{aligned} \tag{19}$$

Water-level fluctuations in both aquifers induced by the leakage can be obtained by the integral of Eq. (14) and (15), respectively, over an area of πR^2. Considering Eqs. (6, 18 and 19) leads to:

$$s^{-} = \xi_1 e^{(-Db)} \lambda_1 \int_0^{2\pi} \int_0^{R^{-}} s_0(r^{-},\theta,f) dr^{-} d\theta , \tag{20}$$

$$s^{+} = -\xi_2 \lambda_1 \int_0^{2\pi} \int_0^{R^{+}} s_0(r^{+},\theta,f) dr^{+} d\theta . \tag{21}$$

The water-level fluctuations in the aquifer are commonly measured by observation wells. r and θ in Eqs. (19-21) are polar coordinates centred on an observation well (Fig. 1c), s^- and s^+ are the water-level fluctuations in the observation wells in the lower and upper aquifers, respectively; R^- and R^+ are the influence radius, over which the stresses can contribute to the water-level fluctuations in observation wells.

If observation wells in both aquifers are located close to each other so that their water-level changes are induced by the same original stresses, then the following equation is satisfied:

$$\int_0^{2\pi} \int_0^{R^{-}} s_0(r^{-},\theta) dr^{-} d\theta = \int_0^{2\pi} \int_0^{R^{+}} s_0(r^{+},\theta) dr^{+} d\theta . \tag{22}$$

Therefore, taking the ratio o f s^- and s^+ gives:

$$s^{-} = -\frac{K^{+}}{K^{-}} e^{-Db} s^{+} . \tag{23}$$

Expressing Eq. (23) in the form of amplitude and phase, gives,

$$A^{-}(f)\exp[i\phi^{-}(f)] = -\frac{K^{+}}{K^{-}} e^{-Db} A^{+}(f)\exp[i\phi^{+}(f)], \tag{24}$$

where $A^{+}(f)$ and $A^{-}(f)$ are the amplitudes, $\phi^{+}(f)$ and $\phi^{-}(f)$ are the phases of leakage-induced water-level signal at frequency f in the upper and lower aquifers, respectively.

By operating the natural logarithm to both sides of Eq. (24) and equating real and imaginary parts, respectively, the quantitative expressions of the hydraulic diffusivity in a three-layered system are:

$$\frac{K_v}{S_s} = \pi f b^2 \Lambda(f)^{-2} , \tag{25}$$

and

$$\frac{K_v}{S_s} = \pi f b^2 \varphi(f)^{-2} . \tag{26}$$

where $\Lambda(f) = \ln(\frac{A^{+}(f)K^{+}}{A^{-}(f)K^{-}})$ and $\varphi(f) = (\phi^{+} + \pi - \phi^{-})$ stand for the amplitude and phase shift of leakage induced water-level signals in the upper and lower aquifers. The hydraulic conductivities (K^{+} and K^{-}) of the aquifers appear in the expression of hydraulic diffusivity of the aquitard (Eq. 25), because the water-level fluctuations in the aquifers are used to infer properties of the aquitard.

The derivation above started from a signal s_0, which represents the original stresses employed in the top aquifer. Alternatively, when an original stress starts in the bottom aquifer, the same expressions for hydraulic diffusivity of the aquitard can be derived.

The derivation assumes that water level propagates instantaneously in the aquifer. Under this assumption, the water-level build-up processes affected by the storage properties of aquifers are ignored. Appendix A assesses impacts of such water-level built-up processes on the expressions of the hydraulic diffusivity, which starts the derivation assuming a uniform plane-wave on the top of the aquitard. The result suggests that the amplitude-based method (Eq. 25) requires the hydraulic parameters in the aquifers explicitly, but this can be escaped in the phase-based method. As fewer parameters are required, the phase-based method (Eq. 26) is proposed in this study as a mean to calculate the hydraulic diffusivity of the aquitard.

2.2 Calculation of phases

The phases under different frequencies are calculated according to the definition of Fourier transform, where the water-level signals in one aquifer are considered as a sum of trigonometric components of different amplitudes, phase shifts and frequencies. Mathematically, this can be expressed as:

$$s(t) = c_0 + \sum_{j=1}^{\infty}\left[a(f_j)\cos(2\pi f_j t) + b(f_j)\sin(2\pi f_j t)\right]. \tag{27}$$

An approximate estimates of $a(f_j)$ and $b(f_j)$ are given as (Boldt-Leppin and Hendry, 2003):

$$a(f_j) = f_0 \sum_{i=0}^{M-1}\left\{\frac{1}{\pi f_j}\frac{s(t_{i+1}) + s(t_i)}{2}[\sin(2\pi f_j t_{i+1}) - \sin(2\pi f_j t_i)]\right\}, \tag{28}$$

$$b(f_j) = f_0 \sum_{i=0}^{M-1}\left\{\frac{1}{\pi f_j}\frac{s(t_{i+1}) + s(t_i)}{2}[\cos(2\pi f_j t_i) - \cos(2\pi f_j t_{i+1})]\right\}, \tag{29}$$

where f_0 is a basic frequency, M is the number of sampling points, and f_j is the frequency considered. f_0 is optimised by comparing observed values of $s(t)$ versus back-calculated $s(t)$, which are calculated by using $a(f_j)$ and $b(f_j)$ resulting from Eqs. (28) and (29) in Eq. (27).

Consequently, the phase at f_j can be calculated by,

$$\phi(f_j) = \arctan[\frac{a(f_j)}{b(f_j)}]. \tag{30}$$

2.3 Selection of frequencies

The solution of hydraulic diffusivity in Eq. (26) is based on the phase-shift of leakage-induced water-level fluctuations. However, in an aquifer, the water-level fluctuations can be influenced by multiple factors (e.g. artificial extraction/injection, barometric pressure, and external recharge). Coherence analysis offers the possibility to identify the frequencies where the leakage- induced signals are dominant.

The coherence can vary from 0 to 1.0, depending on the convolution relationship between the two signals, and is defined as:

$$\kappa_{12}(f)=\frac{\sum_{n=1}^{N}S_{1n}(f)S_{2n}^{*}(f)}{\sqrt{\sum_{n=1}^{N}S_{1n}(f)S_{1n}^{*}(f)}\sqrt{\sum_{n=1}^{N}S_{2n}(f)S_{2n}^{*}(f)}}, \tag{31}$$

where κ is the coherence, * denotes the complex conjugate, N is the number of segments selected in signals $s_1(t)$ and $s_2(t)$. $S_{1n}(f)$ and $S_{1n}(f)$ is the Fourier transform of time series $s_1(t)$ and $s_2(t)$. The coherence is generally calculated using Welch's method (Welch, 1967), and N is selected to be eight in this study, with respect to the default value of the *mscohere* function in the Matlab Signal Processing Toolbox.

The leakage-induced water-level fluctuations in two adjacent aquifers satisfy a convolution relationship (Eq. 1). Hence, the theoretical coherence (Eq. 31) between the leakage-induced water-level fluctuations is 1.0 (Carter, 1987; Padilla and Pulido-Bosch, 1995). However, we could not always find a frequency where the water-level signal is only induced by leakage with a coherence value of exactly 1.0, because the water-level changes induced by different factors interact both linearly or nonlinearly so that leakage-induced signal is possibly interrupted at all frequencies. Hence, it is more realistic to use relatively large coherence values (e.g. larger than 0.6) to identify the frequencies where the hydraulic diffusivity should be calculated. At these frequencies, although the signals are not unambiguously caused by the leakage, it is still reasonable to consider that the leakage is the main factor. The coherence value affects the selection of frequencies, but does not affect the results of hydraulic diffusivity significantly. This will be shown in section 3.1.

2.4 Estimation of K_v

In most field situations, the causal relationship between water-level fluctuations in two aquifers can only be caused by the leakage via their interbedded aquitard. Hence, larger coherence is induced by leakage. However, we cannot rule out that special cases may also lead to a high coherence at certain frequencies. This may occur, for example, when groundwater is extracted in both aquifers with a single pumping well; when the water-level changes in aquifers are induced by tidal or barometric loading; or when there is a common regional groundwater flow affecting both aquifers. In such cases, using the large coherence value to identify the leakage-induced water-level fluctuations is not sufficient. The identified frequencies need to be further checked in order to uniquely estimate K_v.

In addition, the phases calculated by the arctangent function (Eq. 30) range from $-\pi/2$ to $\pi/2$. However, the phases of $\varphi(f_j)$, $\varphi(f_j)+\pi$ and $\varphi(f_j)-\pi$ give the same value in tangent function. This promotes the ambiguities on K_v estimation based on Eq. (26).

A simple method to reduce ambiguity is to pre-estimate K_v of the aquitard according to its lithology and thus producing an approximate K_v range. The impossible values beyond this range are excluded. For example, if large coherences are induced by pumping water in both aquifers, the estimated K_v at these identified frequencies are much higher than the real K_v for the aquitard, because the water-level variations in both aquifers occur almost without time lags.

Furthermore, the ambiguities can be clarified according to the tendency between phases and frequency (Padilla and Pulido-Bosch, 1995). Recalling Eq. (26), in a deterministic aquitard, the phases and frequencies should satisfy a linear log-log relationship:

$$\log\varphi^2 = -(-\log f) + C_0, \tag{32}$$

where C_0 is a constant related to the specific storage and hydraulic conductivity of the aquitard, which can be expressed as:

$$C_0 = -\log(\frac{K_v}{\pi b^2 S_s}), \tag{33}$$

where log represents the logarithm to base 10.

According to Eq. (32), the slope of the linear correlation of $\log\varphi^2$ and $-\log f$ is fixed as -1.0. C_0 is equal to its intercept which can be found by the least square method. Consequently, the value of K_v can be calculated from C_0:

$$K_v = \pi b^2 S_s 10^{-C_0}. \tag{34}$$

3. Case studies

Based on the previous discussion, the steps for estimating K_v can be outlined as:

(1) carrying out coherence analysis of water-level time series measured in the two aquifers adjacent to the aquitard, in order to select the frequencies where K_v should be calculated;

(2) calculation of the phases of water-level time series at the selected frequencies using Eqs. (28-30);

(3) linear regression analysis of the relationship between $-\log f$ and $\log\varphi^2$ to determine C_0 according to Eqs. (32) and (33);

(4) calculation of K_v according to Eq. (34);

(5) use K_v in Eq. (4) to calculate the maximum frequency. The frequencies (selected by coherence analysis) exceeding the maximum frequency should be filtered, and the K_v is recalculated based on the new set of frequencies.

A synthetic case study, in which water-level fluctuations are generated by FELOW model, is used to validate the proposal approach, mainly to investigate the dependence of results on the thickness of the aquifer (with respect to Assumption 4, water-level fluctuations propagating half-spherically in the aquifer), distance of observation wells (with respect to Assumption 5, water-level changes propagating instantaneously in the aquifer), and the domain of applicability of the proposed methodology. Following validation, the methods are applied to a real case in the eastern Eromanga Basin, Australia.

3.1 Simulated example

The numerical modeling software FEFLOW is used to produce synthetic water-level fluctuations in a two-aquifer-one aquitard system within an arbitrary-shaped study area (Fig. 2). The top, bottom, and margins of the system are considered as no-flow boundaries. The hydraulic parameters of each layer in the system are assigned deterministically; hence, the estimates of K_v can be validated. The hydraulic conductivities of the upper and lower aquifer are given as 2 m/d and 5 m/d, respectively, and the specific storage of both aquifers is assigned as 10^{-5} m^{-1}. The hydraulic conductivity of the aquitard is 10^{-4} m/d, and the specific storage is 10^{-4} m^{-1}. Random water-level fluctuations taken in a uniform distribution, varying from -5 to 5 m are input into FEFLOW as a hydraulic-head boundary at point *p* in the upper aquifer (Fig. 2b). These water-level fluctuations are treated as an arbitrary stress occurring in the upper aquifer, and the water-level responses are measured in the observation wells at different locations (Fig. 2b). The time interval of both input and observed water-level time series is one day; hence, K_v is calculated at frequencies less than 1.0 per day, with respect to the period larger than one day. The thicknesses of the lower aquifer and aquitard are fixed as 5 m and 10 m, respectively. In order to describe the flow processes in the aquitard accurately, the aquitard is divided into ten layers and each layer is 1 m.

3.1.1 Influence of aquifer thickness on K_v estimation

Water-level fluctuations in observation wells a_1 and *b* were generated by numerical simulation under different upper aquifer thicknesses (1, 10, 20 and 50 m). Fig. 3a shows the input water-level signal at *p* and water-level fluctuations at *b* induced by the stress at *p*, which indicates that the stress occurring in the upper aquifer induces the water-level changes in the lower aquifer. Hence, there is a causal relationship between water levels in upper and lower aquifer via leakage. Fig. 3b and 3c illustrate the effects of phase calculation using the methodology in section 2.2 for the water-level fluctuations at a_1 and b, respectively. The results show that when the basic frequency (f_0 in Eqs. 28 and 29) is given as 5×10^{-4} per day, the back-calculated water levels compare well with the observed ones. Therefore, phases can be calculated effectively using Eqs. (28-30).

The coherences between water-level fluctuations in the upper and lower aquifer are calculated using the *mscohere* function in Matlab at frequencies smaller than 1.0 per day with an interval of 0.002 per day. As shown in Fig. 4, the coherence increases with the thickness of the upper aquifer, but quickly stabilise.

The value of C_0 is calculated according to Eqs. (32) and (33), and the results are illustrated in Fig. 5. The scatter plots of $-\log f$ and $\log\varphi^2$ are fitted linearly by the least square method, and the slope of the trend line is fixed to -1.0 according to Eq. (32). Fig. 5a-5d demonstrate that the square correlation coefficient (R^2) between predicted and output $\log\varphi^2$ increase with the thickness of the upper aquifer, but the value of C_0 calculated under different aquifer thicknesses does not vary significantly and compares well with the theoretical value (2.4972, which is calculated for K_v=10^{-4} m/d according to Eq. 33).

In the above cases, the impact of aquifer-thickness on coherence comes from the top boundary of the upper aquifer. When this aquifer is thin, the top boundary is close to the aquitard and produces stronger interruption on the leakage-induced water-level signals. Therefore, coherence presents a smaller value than 1.0. Relating the coherence with R^2 indicates that the small coherence results in a weak linear correlation between $-\log f$ and $\log\varphi^2$. However, since a linear trend between frequencies and phases can be found at relatively higher coherences, the results of C_0 and K_v do not change significantly due to the thickness of the aquifer. Therefore, it is safe to ignore the influence of aquifer-thickness on propagation in assumption 4, as long as the sufficient number of large coherences can be presented to identify the frequencies, and the linear trend between $-\log f$ and $\log \varphi^2$ can be determined by the least square method.

3.1.2 Influence of observation-well distances

Another assumption used in the derivation ignores the time lags for water-level signals transferring in the aquifer. In order to validate this assumption, we calculate the coherence based on the water-level changes in observation wells of different distances: a_1 and b, 0 m; a_2 and b, 10 m; a_3 and b, 20 m; a_4 and b, 90 m; a_5 and b, 190 m (Fig. 2b). Fig. 6 shows that the coherence cannot reach 1.0, because the leakage-induced water-level signals are interrupted by the other factors (artificial stress and boundary conditions). Fig. 6b and 6c indicates that coherence increases slightly when the distance between observation wells increases. This is because a_1 is closer to the imposed stress, the leakage-induced water-level signal is more strongly interrupted and the coherence between a_1 and b is lower than the coherence calculated on the basis of the other water-level pairs.

Fig. 7 shows the C_0 and K_v calculated from different pairs of water-level measurements. The result suggests that K_v increases with the distance between observation wells (Fig. 7b), because the water-level in these synthetic cases is originally induced by the artificial stress at p (Fig. 2). There is a time lag for the signal transferring from p to the observation well. The time lag between, for example, b and a_5 is smaller than the one between b and a_1. Therefore, the K_v estimated by water levels measured at b and a_5 is larger than b and a_1. The differences between the estimations of K_v based on water-level measurement at $a_{1\text{-}5}$ and b represent the errors introduced by assuming that the water-level propagate instantaneously in the aquifer. Fig. 7b examines these errors graphically, and the results indicate that within a distance of 200 m, the hydraulic conductivity is not altered significantly (from 0.9900 to 1.0735 $\times 10^{-4}$ m/d) and approaches a constant when the distance keeps increasing. Hence, it is realistic to assume that the water level propagates instantaneously in the aquifers, and the observation wells are allowed to be separated by a horizontal distance. But the two observation wells should not be so far away from each other that they are affected by completely different stresses, otherwise, the relationship shown in Eq. (22) does not firmly stand.

Figs. 4-7 suggest that both thickness of the aquifers and the distance of observation wells affect the coherence value. The coherence variation affects the correlation coefficients between the predicted and output $\log\varphi^2$. In general, low coherence values lead to more scattered plots of $-\log f$ versus $\log\varphi^2$ with low correlation coefficients. However, since a linear trend line can be found based on these scatter plots, the results of C_0 and K_v are not impacted significantly, and can compare very well with the theoretical value. Hence, both assumptions 4 and 5 are realistic, and the proposal methods can calculate the vertical hydraulic conductivity of the aquitard.

3.1.3 Casual relationship

The proposed method presumes that there is a casual relationship between water-level fluctuations in two adjacent aquifers (Assumption 3).This assumption requires that the water-level signal can penetrate the aquitard effectively. Fig. 8 illustrates two factors that can affect this causal relationship: the energy of water-level signal in the aquifers and the decay rate in the aquitard.

Fig. 8a repeats the results for the synthetic case that the thickness of the upper aquifer is 20 m, the aquitard thickness is 10m, the distance between two observation wells is zero and the input signal at p is the same as in Fig. 3a. The case in Fig. 8b exaggerates the frequencies and decreases the amplitude of input signal used in the case of Fig. 8a. Such frequency and amplitude changes can reduce the energy of the input water-level signal. The result of coherence analysis of water-level changes at a_1 and b is shown in Fig. 8b$_2$. As shown, smaller coherences between the frequencies of 0- 0.15 are presented, that only 27 frequencies having the coherences larger than 0.70 when compared to 38 frequencies corresponding the coherences larger than 0.80 in Fig. 8a$_2$. Calculating the phases at these 27 frequencies, and plotting the logarithm transformed phases and frequencies in Fig. 8b$_3$, yield a linear relationship with R^2 of 0.6289, and a K_v near to 10^{-4} m/d. Though the result of K_v does not change significantly, both the low coherence and small R^2 indicate that weak water-level fluctuations in one aquifer result in the weak leakage-induced water-level variations, which can be easily interrupted by other factors (such as the top or bottom boundary of the aquifer in this case). If the water-level fluctuations are too weak, it is possible that no large coherence can be found or no linear relationship between frequencies and phases can be established at the selected frequencies. In this situation, the C_0 and K_v cannot be calculated.

The case in Fig. 8c uses the same input signal as the one in Fig. 8a, but the thickness of the aquitard is given as 20 m. Fig. 8c$_1$ shows that the output signal (observed at *b*) is flatter than that in Fig. 8a$_1$ due to the stronger decay during the signal penetrating the aquitard. As a consequence, lower coherences and very small R^2 (0.0858) are shown in Fig. 8c$_2$ and c$_3$, respectively. The small R^2 indicates that linear correlation between phase and frequencies in Fig. 8c$_3$ may induce large errors to estimate K_v. If the aquitard is too thick, no signal can penetrate the aquitard effectively and the causal relationship between aquifers cannot be satisfied. Therefore, the proposed method cannot work.

Eq. (4) provides a theoretical view of the causal relationship, which leads to an expression of the maximum frequency ($f_{\max}$) allowing the calculation of K_v. Prior to estimation of $f_{\max}$, we use the synthetic case in Fig. 8a to select the energy effectiveness (*E*) and characteristic coefficient (*d*) (Eq. 4), because Fig. 8a has shown that our proposed approach works well in this synthetic case. As both *E* and *d* are used as variables independent to the aquitard properties (thickness and hydraulic diffusivity), the results from such a specific case can be applied to the other cases.

E is selected according to the coherence distribution in Fig. 8a$_2$. For the signals at the low frequencies (<0.03 in this synthetic case), the water-level fluctuation is unclear. Although the water-level signal can penetrate the aquitard effectively, the signal energy before decaying in the aquitard is too weak to enable the causal relationship to be detected and the coherence will be low. In contrast, at the large frequencies (e.g. > 0.12 herein), though the signal energy in the aquifer can be very large, it diverges too much in the aquitard and cannot penetrate the aquitard effectively. As a result, the large coherence and detectable causal relationship between water levels in two aquifers appear in a frequency range of 0.03- 0.13.

As shown in Fig. 9a and 9b, both *d* and $f_{\max}$ reduce with increases of *E*. If *E* is larger than 3%, $f_{\max}$ is smaller than 0.03. But all the large coherences (>0.8) in Fig. 8a$_2$ are not within the frequencies lower than this $f_{\max}$. Hence, *E* should be selected as a value smaller than 3%.

E reducing from 3% to 0.2% corresponds to $f_{\max}$ increases from 0.03 to 0.12. K_v gets close to the theoretical value (10^{-4} m/d), and R^2 increases from 0.032 to a value around 0.83. If *E* becomes lower than 0.2%, $f_{\max}$ becomes larger than 0.12, but both K_v and R^2 do not change with *E*. Although all the large coherences locate at the frequencies lower than this $f_{\max}$, $f_{\max}$ is overestimated which cannot play a role to restrict the frequencies for the calculation of $K_{v.}$

Hence, we select *E* to be 0.2%, and *d* is estimated as 12. Once *E* and *d* are determined, the $f_{\max}$ can be calculated to examine the frequencies used in the calculation of K_v. For the harmonic signals at those frequencies larger than $f_{\max}$, only less than 0.2% of its energy can penetrate the aquitard. At these frequencies, even though some large coherences are presented, they are more likely induced by the unexpected noisy in this signal rather than the leakage. Hence, K_v should not be calculated at these frequencies. Because $f_{\max}$ is determined by hydraulic diffusivity, which is a variable resulting from the calculations, $f_{\max}$ can only be used as a posteriori validation.

Furthermore, the discussion of f_{max} can suggest the domain of applicability of the proposed method. For example, according to Eq. (4), the f_{max} would change from 12 to 0.0012 if the thickness of the aquitard increases from 1 to 100 m in the synthetic case. When the aquitard thickness is 20 m, the f_{max} is 0.03. This indicates that in the case of Fig. 8c, K_v can only be calculated at the frequencies lower than 0.03. However, as shown in Fig. 8c$_2$, no large coherences are shown for the frequencies in this range, hence, the proposed method cannot work. As to the high coherences in Fig. 8c$_2$ at the frequency larger than 0.03, it is likely to be induced by the noisy, and so a very weak linear correlation between frequencies and phases is shown in Fig. 8c$_3$.

The proposed method may not work when the aquitard thickness exceeds certain upper limit. In this synthetic case, the value of this upper limit is 20 m. But upper limit of aquitard thickness also depends on the hydraulic diffusivity of the aquitard. In the situation of higher hydraulic diffusivity, the proposed method can be applied to a thicker aquitard.

In another two cases in Fig. 8, the thickness of the aquitard is 10 m, and the f_{max} is estimated to be 0.12. Hence, the K_v should be calculated at frequencies lower than 0.12, with respect to a –log(f) larger than 0.92. All the frequencies used in K_v calculation in Fig. 8b$_3$ are within this range, but in Fig. 8a$_3$, one frequency exceeds f_{max} (where –log(f)=0.88). After removing this frequency, K_v is recalculated; however, the result does not change significantly.

3.2 Real case study

3.2.1 Materials

The proposed methods are applied to the multilayered leaky aquifer system of the eastern Eromanga Basin, which forms part of the Great Artesian Basin (Fig. 10). The fluvial and lacustrine sediments of the Eromanga Basin (Hutton to Hooray aquifer) were deposited in the Early Jurassic and Late Cretaceous period, and are covered by a thick sequence of the

Cretaceous shallow marine sediments of the Rolling Downs Group (Habermehl, 1980; Idnurm and Senoir, 1978).

The aquifers and aquitards are defined based on lithology, hydraulic properties and thickness of the formations, and are summarized in Table 1. This test case focuses on a five-layered leaky system composed of the Hooray, Adori and Hutton aquifers separated by the Westbourne and Birkhead aquitards (Fig. 10).

The aim of this study is to estimate the K_v for the Westbourne and Birkhead aquitards based on water-level fluctuations in three adjacent aquifers. Water-level measurements in the three aquifers were extracted from the groundwater database of the Department of Environment and Resource Management Queensland (DERM). Three observation wells with water-level measurements from 01/01/1919 to 2/10/1992 are selected in the Hooray, Adori and Hutton aquifers. The observation wells are approximately at the same location (Fig. 10). Water levels are normalized so that they have a zero mean and a unit standard deviation (Fig. 11). Because the time intervals at each time series are greater than 10 days, K_v is calculated at frequencies less than 0.1 per day, with respect to a period larger than 10 days. In addition, the water-level time series in three wells are modified into the same sampling resolution of 10 days. The missing data are interpolated linearly, for the purpose that the Fourier transforms of these modified time series are still controlled by the data that are actually measured.

3.2.2 Estimates of hydraulic conductivity

Before calculating K_v, the specific storage of the aquitards is estimated based on the downhole sonic and density log data in Bonnie and Milo drillholes (Fig. 10). The methodology is presented in appendix B. As a result, the specific storage for the Westbourne and Birkhead aquitard is 5.95 and 5.8 $\times 10^{-7}$ m^{-1}, respectively.

In order to select the frequencies for the calculation of K_v, coherences are calculated at 100 frequencies between 0 and 0.1 with an interval of 0.001 per day. Fig. 12 displays the frequencies where large coherences (>0.6) are presented. According to Fig. 12, K_v in both Westbourne and Birkhead aquitards are calculated at fourteen frequencies.

Based on the frequencies identified by the coherence analysis, the relationship between frequencies and phase shift are investigated according to Eq. (32), and the C_0 values are displayed in Fig. 13. Recalling Eq. (34), K_v of the Westbourne and Birkhead aquitards are estimated to be 2.23 $\times 10^{-5}$ m/d and 4.65 $\times 10^{-5}$ m/d, respectively.

Making use the resulted hydraulic conductivity and specific storage in Eq. (4) leads to the maximum frequency for the Westbourne and Birkhead aquitards, which are roughly 0.059 and 0.075 per day, respectively. Recalling the frequencies used in calculation (Fig. 12), there are three frequencies (0.0889, 0.0619, 0.0618 and 0.0944, 0.082, 0.0795) exceeding the maximum frequency in the Westbourne and Birkhead aquitards, respectively. After removing these frequencies, the K_v is recalculated in both aquifers; as a result, K_v is revised as 2.17×10^{-5} m/d and 4.31×10^{-5} m/d, respectively.

To our knowledge, there are no studies which have been carried out to estimate K_v in the Westbourne and Birkhead aquitards in the Eromanga Basin. Some results were reported during petroleum exploration and hydrogeological studies in the adjacent Surat Basin (Fig. 10), which was deposited in the similar paleo-environment as the Eromanga Basin. The value of K_v for the Westbourne aquitard in the Surat Basin were reported to be 2.0×10^{-6} -2.0×10^{-5} m/d in a numerical groundwater flow model (USQ, 2011). The harmonic hydraulic conductivity of the Birkhead aquitard was estimated to be 2.04×10^{-4} m/d according to permeability- measurements of 119 cores by Alexander and Boult (2011). The K_v estimated in this study are comparable to those reported values.

5. Summary and conclusion

The major contributions of this paper are summarized as follows.

1. The harmonic analysis approach to estimate the vertical hydraulic conductivity (K_v) of an aquitard was developed in a multilayered leaky system. K_v can be calculated based on arbitrary water-level fluctuations measured in the aquifers. Both the amplitude- and phase-based expression of K_v were given analytically. Because the phase-based method does not require the hydraulic parameters within the aquifers explicitly, it is proposed as a more convenience method to determine K_v than the amplitude-based method.

2. The arbitrary water-level fluctuations in the aquifer maybe caused by multiple factors. The condition for application of harmonic analysis method is that the aquitard is leaky and leakage causes measurable water-level changes in the two adjacent aquifers. The coherence function was employed to identify the frequencies where the leakage-induced water-level fluctuations dominate, because the convolution correlation between leakage-induced water-level changes leads to a coherence approaching 1.0. K_v were then calculated at these frequencies.

3. A robust method to calculates K_v used the intercept of the linear logarithm correlation between phases (φ) and frequencies (f). The slope of the linear relationship was fixed as -1. The intercept was estimated based on the least square method.

4. A synthetic case was used to validate the proposed methods. The results indicated that both the distance of observation wells and thickness of the aquifer affect the coherence value. However, the coherence value can only impact the correlation coefficient between predicated and output $\log\varphi^2$. The intercept (C_0), and so the K_v, did not change with variations of coherences. Therefore, it is allowed that the coherences cannot reach 1.0, as long as the relatively large coherences can be presented and the linear correlation between phases and frequencies can be determined.

5. The proposed method was applied to calculate K_v of the Westbourne and Birkhead aquitards in Eromanga Basin, Australia. The results are comparable with the reported values.

The proposal methods can estimate K_v, however, with certain limitations:

(1) A causal relationship must exist between water-level fluctuations in both adjacent aquifers, which is caused by the leakage via the interbedded aquitard. If this is not satisfied, at least one set of water-level measurements in the aquitard is required.

(2) A significant permeability-contrast (> 100) between aquifers and aquitard are required to enable the assumption that the groundwater flows vertically in the aquitard;

(3) Aquifers and aquitard can be approximated as homogeneous, otherwise, the resulted K_v represents an average property of the aquitard.

Appendix A

The derivation of hydraulic diffusivity in section 2.1 ignored the influences of the water-level build-up process relating to storage properties of the aquifer. In order to investigate the impact of such a process on the quantitative expression of the hydraulic diffusivity, we illustrate a case where the initial signal s_0 is added uniformly on top of the aquitard, which can be considered as a plane source. Hence, no lateral propagation would occur when the signal reaches the aquifers.

The signal s_0 transfers through the aquitard and before it reaches the lower aquifer, the signal in the aquitard can be expressed by,

$$s(f) = s_0(f)e^{(-Dz)}. \qquad \text{A-1}$$

Once the signal from the aquitard reaches the lower aquifer, the water-level built-up process in lower aquifer can be derived from,

$$-\frac{ds}{dz} = \frac{1}{\eta^-}\frac{\partial s_1^-}{\partial t}, \qquad \text{A-2}$$

where $\eta^- = \dfrac{K_v}{\mu^-}$ and μ^- is storage coefficient of the lower aquifer.

As a result, in frequency domain,

$$s_1^- = \frac{D}{(D^-)^2} s_0 e^{(-Db)}, \qquad \text{A-3}$$

where $D^- = \sqrt{\frac{\pi f}{\eta^-}}(1+i)$.

Similarly, water-level build-up in the upper aquifer with respect to s_0 can be expressed as,

$$s_1^+ = -\frac{D}{(D^+)^2} s_0, \qquad \text{A-4}$$

where $D^+ = \sqrt{\frac{\pi f}{\eta^+}}(1+i)$, $\eta^+ = \frac{K_v}{\mu^+}$, μ^+ is the storage coefficient within the upper aquifer.

After defining $\xi_1 = \frac{D}{(D^-)^2}$ and $\xi_2 = \frac{D}{(D^+)^2}$, the water levels in each aquifer can be expressed by the same formulae as Eqs. (14) and (15) and the relationship between leakage-induced water levels satisfy:

$$A^-(f)\exp[i\phi^-(f)] = -\frac{\mu^+}{\mu^-} e^{-Db} A^+(f)\exp[i\phi^+(f)], \qquad \text{A-5}$$

Operating the logarithm on both sides of Eq. (A-5) and equating real and image parts respectively, gives,

$$\frac{K_v}{S_s} = \pi f b^2 \left[\ln\left(\frac{A^+\mu^+}{A^-\mu^-}\right)\right]^{-2}, \qquad \text{A-6}$$

$$\frac{K_v}{S_s} = \pi f b^2 (\phi^+ + \pi - \phi^-)^{-2}. \qquad \text{A-7}$$

Recalling the results (Eq. 25) in section 2.1, the amplitude-based equation is affected explicitly by both the storage coefficient and hydraulic conductivity of the aquifers.

Appendix B

The specific storage can be inferred from geophysical log data, including sonic and density logging data, based on the definition (Freeze and Cherry, 1979):

$$S_s = \rho_w g(\alpha + \psi\beta) = \rho_w g M \qquad \text{B-1}$$

where ρ_w is the density of the water(1000kg/m^3), g is the acceleration of gravity (9.8m/s^2), α is the matrix compressibility, ψ is the porosity, β is the fluid compressibility and M is the bulk compressibility of the aquitards.

M can be estimated from the sonic wave velocity by (Berryman, 2000; Morin, 2005):

$$M = \frac{3}{\rho_b(3V_p^2 - 4V_s^2)}, \qquad \text{B-2}$$

where ρ_b is the bulk density which can be obtained from the density log data, V_p is the compressional wave velocity recorded during the sonic log, V_s is the shear wave velocity, which is difficult to measure directly from sonic log, but commonly estimated (Castagna et al., 1985) by:

$$V_p = 1.16V_s + 1.36, \qquad \text{B-3}$$

Substituting Eqs. (B-2) and (B-3) into (B-1), the specific storage can be estimated.

Acknowledgements

Funding support for this study came from China Scholarship Council, and financial support from Exoma Energy Ltd is also gratefully acknowledged. Denial Owen and Matthias Raiber are thanked for their suggestions and proofreading on the manuscript. We thank two anonymous reviewers for their helpful comments.

Reference

Alexander, E.M., Boult, P.B., 2011. Petroleum geology of South Australia , Volume 2: Eromanga Basin, Chapter 11: Reservoirs and seals. 141-147.

Arns, C.H., Knackstedt, M.A., Pinczewski, M.V., Lindquist, W.B., 2001. Accurate estimation of transport properties from microtomographic images. Geophys. Res. Lett., 28(17): 3361-3364.

Berryman, J.G., 2000. Seismic velocity decrement ratios for regions of partial melt in the lower mantle. Geophys. Res. Lett., 27(3): 421-424.

Boldt-Leppin, B.E.J., Hendry, J.M., 2003. Application of Harmonic Analysis of Water Levels to Determine Vertical Hydraulic Conductivities in Clay-Rich Aquitards. Ground Water, 41(4): 514-522.

Carter, G.C., 1987. Coherence and time delay estimation. Proceedings of the IEEE, 75(2): 236-255.

Castagna, J.P., Batzle, M.L., Eastwood, R.L., 1985. Relationships between compressional-wave and shear-wave velocities in clastic silicate rocks. Geophysics, 50(4): 571-581.

Clauser, C., 1992. Permeability of crystalline rocks. Eos, Transactions American Geophysical Union, 73(21): 233-238.

Dagan, G., 1989. Flow and transport in porous formations. Springer-Verlag, 463 pp.

Detournay, E., 1993. Fundamentals of Poroelasticity, in Linear Elastic Diffusive Solids. Analysis and Design Methods, 2: 113.

Eaton, T.T., Bradbury, K.R., 2003. Hydraulic transience and the role of bedding fractures in a bedrock aquitard, southeastern Wisconsin, USA. Geophys. Res. Lett., 30(18): 1961.

Freeze, R.A., Cherry, J.A., 1979. Groundwater. Presentice-Hall, Englewood Cliffs, New Jersey, 604 pp.

Habermehl, M.A., 1980. The Great Artesian Basin. BMR Journal of Australian Geology and Geophysics, 5: 9-38.

Hantush, M.S., 1960. Modification of the Theory of Leaky Aquifers. J. Geophys. Res., 65(11): 3713-3725.

Hantush, M.S., Jacob, C.E., 1955. Non-steady Green’s functions for an infinite strip of leaky aquifer. Am. Geophys. Union Trans., , 36(2): 101-102.

Hart, D.J., Bradbury, K.R., Feinstein, D.T., 2005. The vertical hydraulic conductivity of an aquitard at two spatial scales. Ground Water, 44(2): 201-211.

Herrera, I., Figueroa V, G.E., 1969. A Correspondence Principle for the Theory of Leaky Aquifers. Water Resources Research, 5(4): 900-904.

Idnurm, M., Senoir, B.R., 1978. Palaeomagnetic ages of late Cretaceous and Tertiary weathered profiles in the Eromanga Basin, Queensland. Palaeogeography, Palaeoclimatology, Palaeoecology, 24(4): 263-277.

Larocque, M., Mangin, A., Razack, M., Banton, O., 1998. Contribution of correlation and spectral analyses to the regional study of a large karst aquifer (Charente, France). Journal of Hydrology, 205(3): 217-231.

Morin, R.H., 2005. Hydrologic properties of coal beds in the Powder River Basin, Montana I. Geophysical log analysis. Journal of Hydrology, 308(1–4): 227-241.

Neuman, S.P., Gardner, D.A., 1989. Determination of Aquitard/Aquiclude Hydraulic Properties from Arbitrary Water-Level Fluctuations by Deconvolution. Ground Water, 27(1): 66-76.

Neuman, S.P., Witherspoon, P.A., 1968. Theory of flow in aquicludes adjacent to slightly leaky aquifers. Water Resour. Res., 4(1): 103-112.

Neuman, S.P., Witherspoon, P.A., 1969a. Applicability of Current Theories of Flow in Leaky Aquifers. Water Resour. Res., 5(4): 817-829.

Neuman, S.P., Witherspoon, P.A., 1969b. Theory of Flow in a Confined Two Aquifer System. Water Resour. Res., 5(4): 803-816.

Neuman, S.P., Witherspoon, P.A., 1972. Field determination of the hydraulic properties of leaky multiple aquifer systems. Water Resour. Res., 8(5): 1284-1298.

Padilla, A., Pulido-Bosch, A., 1995. Study of hydrographs of karstic aquifers by means of correlation and cross-spectral analysis. Journal of Hydrology, 168(1–4): 73-89.

Remenda, V.H., van der Kamp, G., 1997. Contamination from Sand-Bentonite Seal in Monitoring Wells Installed in Aquitards. Ground Water, 35(1): 39-46.

Schulze-Makuch, D., Carlson, D.A., Cherkauer, D.S., Malik, P., 1999. Scale Dependency of Hydraulic Conductivity in Heterogeneous Media. Ground Water, 37(6): 904-919.

Timms, W., Hendry, M., 2008. Long-Term Reactive Solute Transport in an Aquitard Using a Centrifuge Model. Ground Water, 46(4): 616-628.

USQ, 2011. Preliminary assessment of cumulative drawdown impacts in the Surat Basin Associated with the coal seam gas industry: Investigation of parameters and features for a regional model of Surat Basin coal seam gas development. University of Southern Queensland, Brisbane, 50 pp.

van der Kamp, G., 2001. Methods for determining the in situ hydraulic conductivity of shallow aquitards – an overview. Hydrogeology Journal, 9(1): 5-16.

Welch, P., 1967. The use of fast Fourier transform for the estimation of power spectra: A method based on time averaging over short, modified periodograms. Audio and Electroacoustics, IEEE Transactions on, 15(2): 70-73.

Wolff, R.G., 1970. Field and laboratory determination of the hydraulic diffusivity of a confining bed. Water Resources Research, 6(1): 194-203.

Captions

Fig. 1. Schematic map showing (a) a three-layered leaky aquifer system, (b) the signal processes in the leaky system, and (c) plan view of a source s_0 occurring at an area dA and contributing to water-level fluctuation in observation well. The total water-level fluctuation in the observation well can be calculated using the integral of the contribution of s_0 at the area of πR^2, where R represents the influence radius. Of note, the polar coordinate system in (b) centred at original stress, whereas in (c) centred at observation well.

Fig. 2. (a) Plan view of the study area and boundary conditions, and (b) cross-section view of the leaky system and locations of artificial stress and observation wells. The thickness of upper aquifer varies at 1, 10, 20 and 50 m in order to assess the influence of the aquifer thickness on the estimation of K_z.

Fig. 3. (a) The arbitrary water-level fluctuations at p and water-level responses in the lower aquifer at b; (b) and (c) comparing the observed water levels at a_1 and b, respectively, versus the back-calculated water levels by methodology in section 2.2. Thickness of the upper aquifer is 50 m.

Fig. 4. (a) Coherences between water-level signals measured in observation wells a_1 and b, and (b) blow-up of the high coherences (> 0.8) at frequencies between 0 - 0.15 d^{-1}.

Fig. 5. Estimates of C_0 based on water-level fluctuations within the system of different aquifer thicknesses: (a) 1m, (b) 10 m, (c) 20m and (d) 50 m. The theoretical value of C_0=2.4972 with respect to K_z=0.0001 m/d, and the square of correlation coefficient (R^2) are also indicated.

Fig. 6. Coherence between water levels measured in the lower (at b) and upper aquifer (at a_1, a_2, a_3, a_4, a_5). The distance between observation wells in the two aquifers is 0, 10, 20, 90 and 190 m.

Fig. 7. (a) Linear correlation between frequency and phase shift, (b) values of C_0 reducing with increasing distance between observation wells and (c) the correlation coefficients of the linear regression model. The vertical hydraulic conductivities are also marked in (b).

Fig. 8. Calculation of K_v for different cases: (a) the aquitard thickness is 10 m, (b) the aquitard thickness is unchanged, but the energy of input signal at *p* is reduced, (c) the energy of input signal is unchanged, but the thickness of the aquitard is enlarged to be 20 m. *f* is the frequencies of the arbitrary water-level signal input at *p*, *A* is the amplitudes of this signal. Unit of K_v is 10^{-4} m/d.

Fig. 9. Large energy effectiveness leads to (a) small maximum frequency, (b) small characteristic coefficient, (c) large error in K_v calculation, and (d) small correlation coefficient,

Fig. 10. Location of the study area and the structure of the multilayered leaky system that is being investigated.

Fig. 11. Water level data plotted against duration from 01/01/1919 to 2/10/1992 for (a) the Hooray aquifer, (b) Adori aquifer and (c) Hutton aquifer.

Fig. 12. Plots of the frequencies with higher coherence values for (a) Westbourne aquitard and (b) Birkhead aquitard.

Fig. 13. Plots of the log-log relationship between frequency and phase shift for (a) Westbourne aquitard and (b) the Birkhead aquitard.

Figure-1

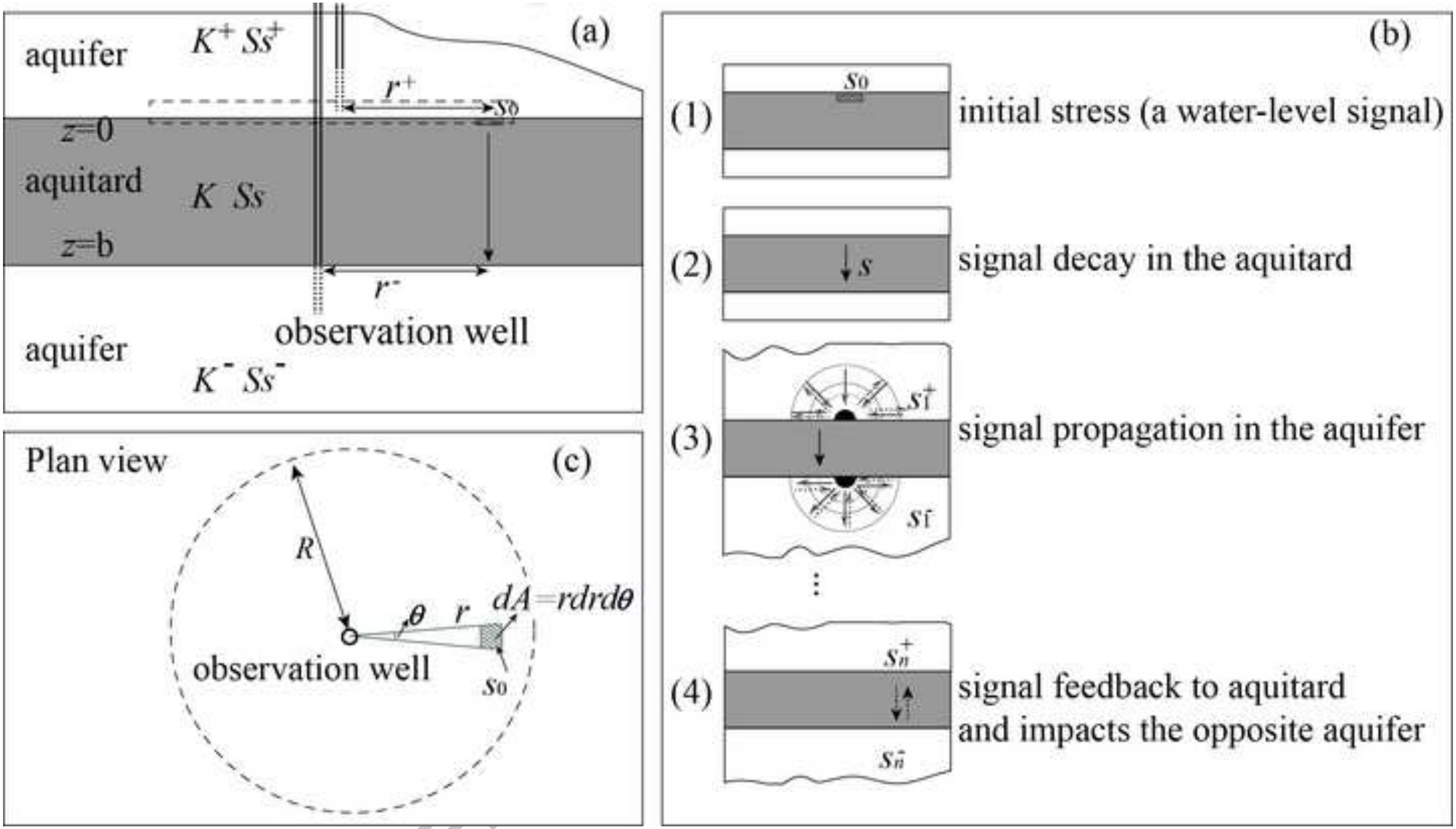

(a)
aquifer
K^+ Ss^+
r^+
s_0
z=0
aquitard
K Ss
z=b
r^-
observation well
aquifer
K^- Ss^-
(b)
(1)
s_0
initial stress (a water-level signal)
(2)
s
signal decay in the aquitard
(3)
s_1^+
signal propagation in the aquifer
s_1^-
(4)
s_n^+
signal feedback to aquitard
and impacts the opposite aquifer
s_n^-
Plan view
(c)
R
θ
r
$dA=rdrd\theta$
observation well
s_0

Figure-2

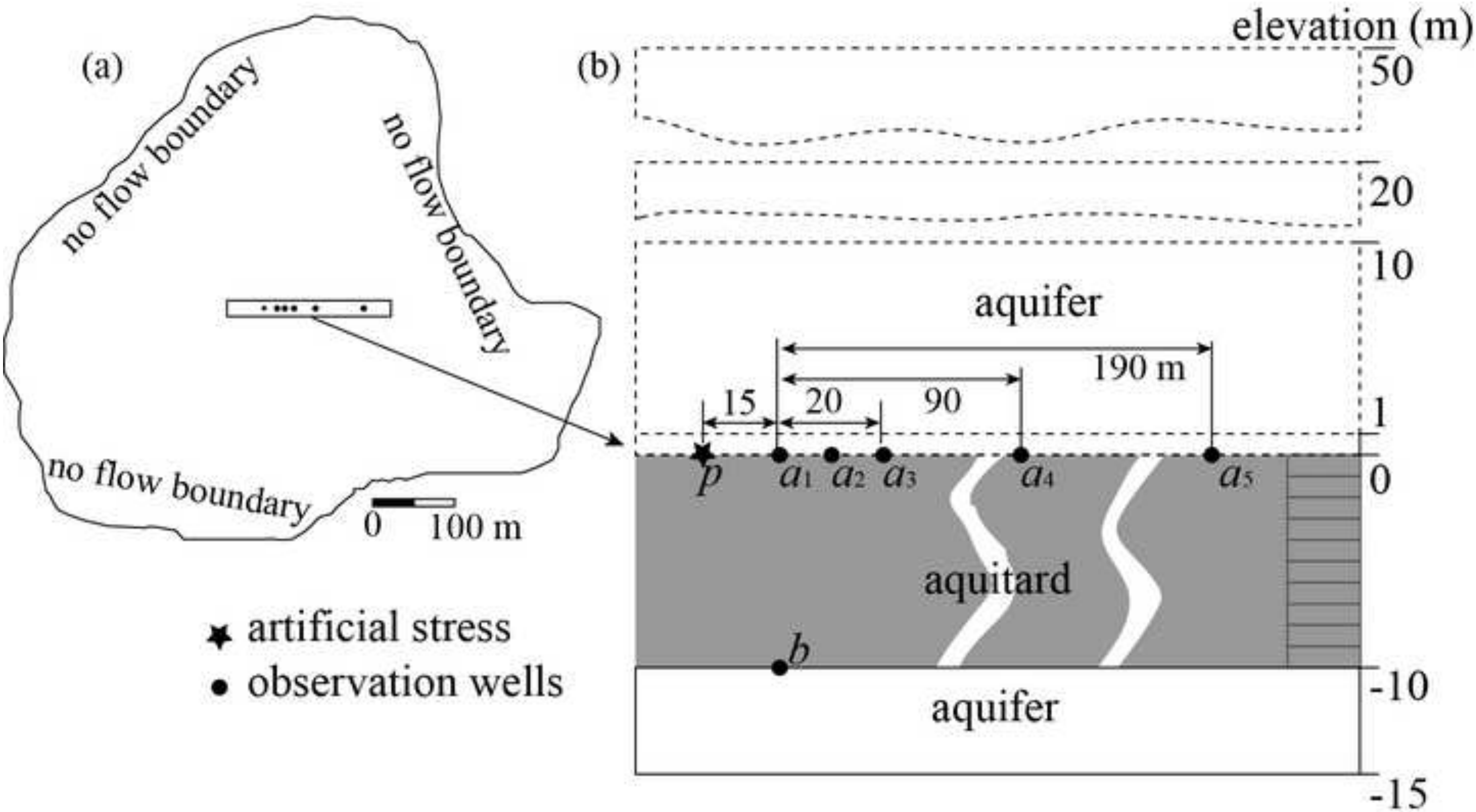

(a)
no flow boundary
no flow boundary
no flow boundary
0
100 m
artificial stress
observation wells
(b)
elevation (m)
50
20
10
1
0
-10
-15
aquifer
190 m
90
20
15
p
a_1
a_2
a_3
a_4
a_5
aquitard
b
aquifer

Figure-3

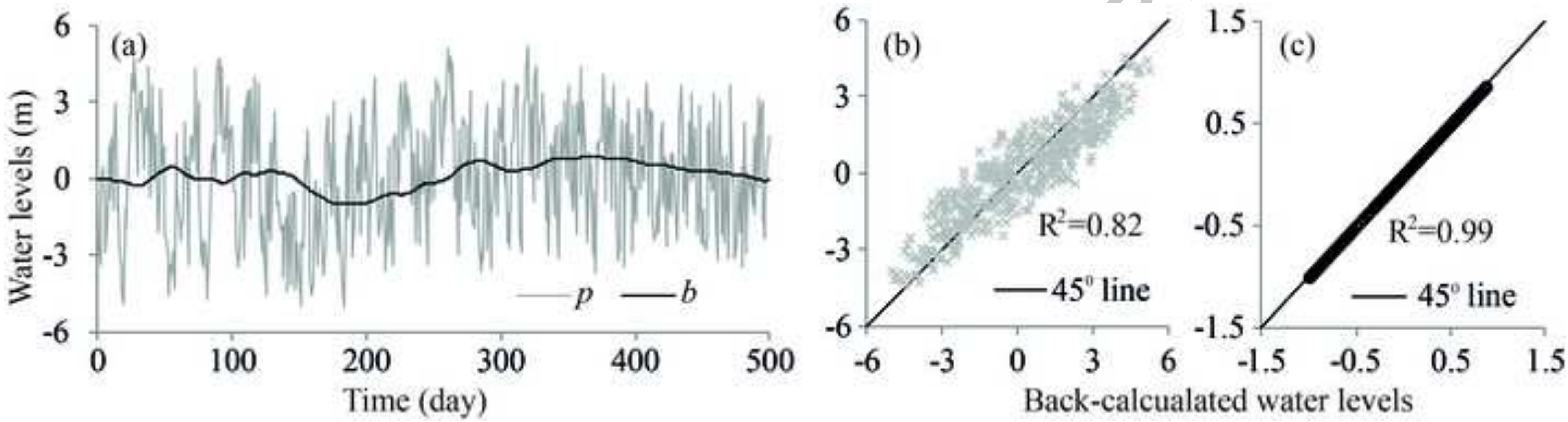
6
3
0
-3
-6
Water levels (m)
(a)
p
b
0
100
200
300
400
500
Time (day)
(b)
R²=0.82
45° line
-6
-3
0
3
6
(c)
1.5
0.5
-0.5
-1.5
R²=0.99
45° line
Back-calcualated water levels

Figure-4

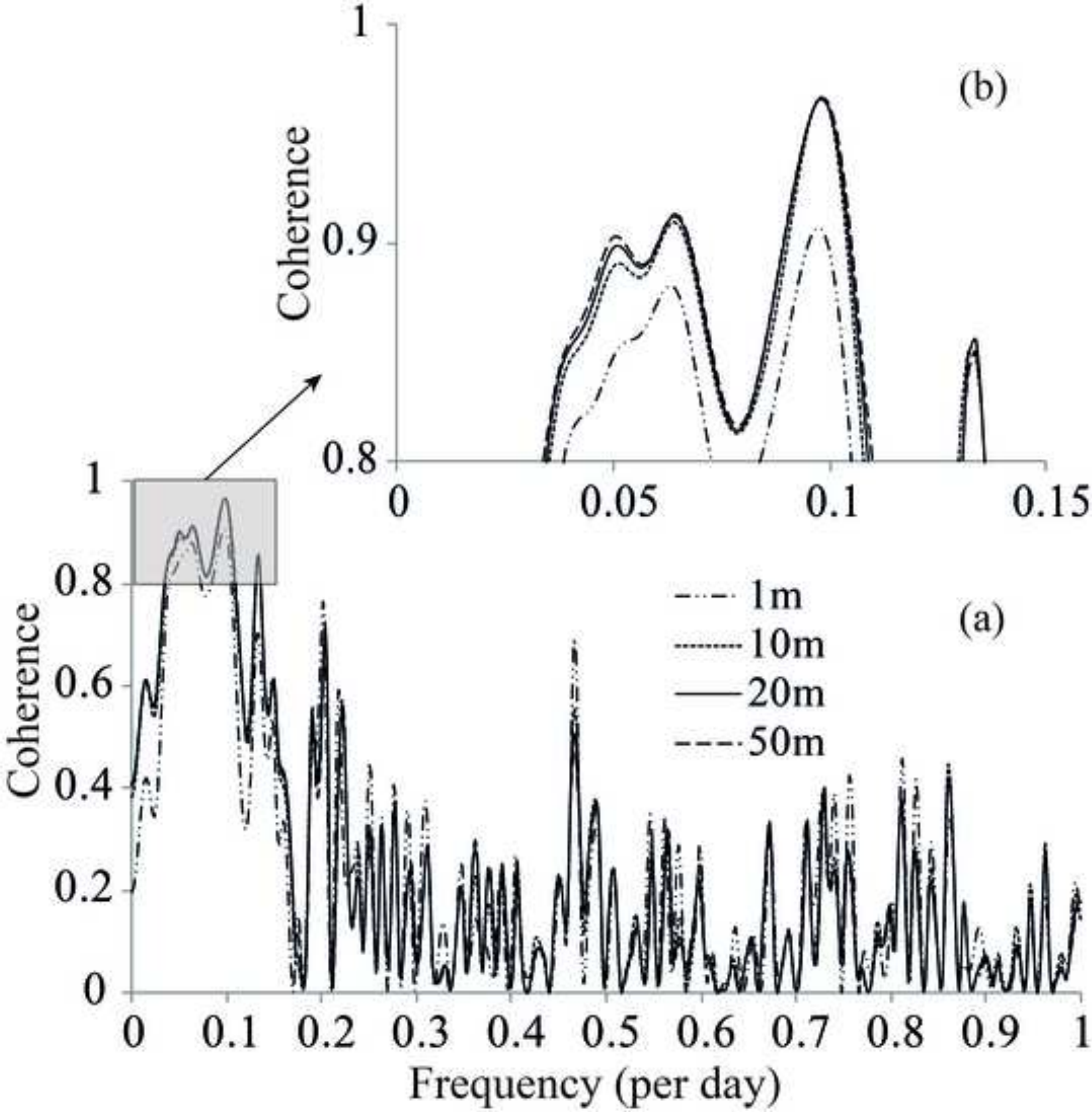
(b)
Coherence
1
0.9
0.8
0
0.05
0.1
0.15
(a)
Coherence
1
0.8
0.6
0.4
0.2
0
0
0.1
0.2
0.3
0.4
0.5
0.6
0.7
0.8
0.9
1
Frequency (per day)
1m
10m
20m
50m

Figure-5

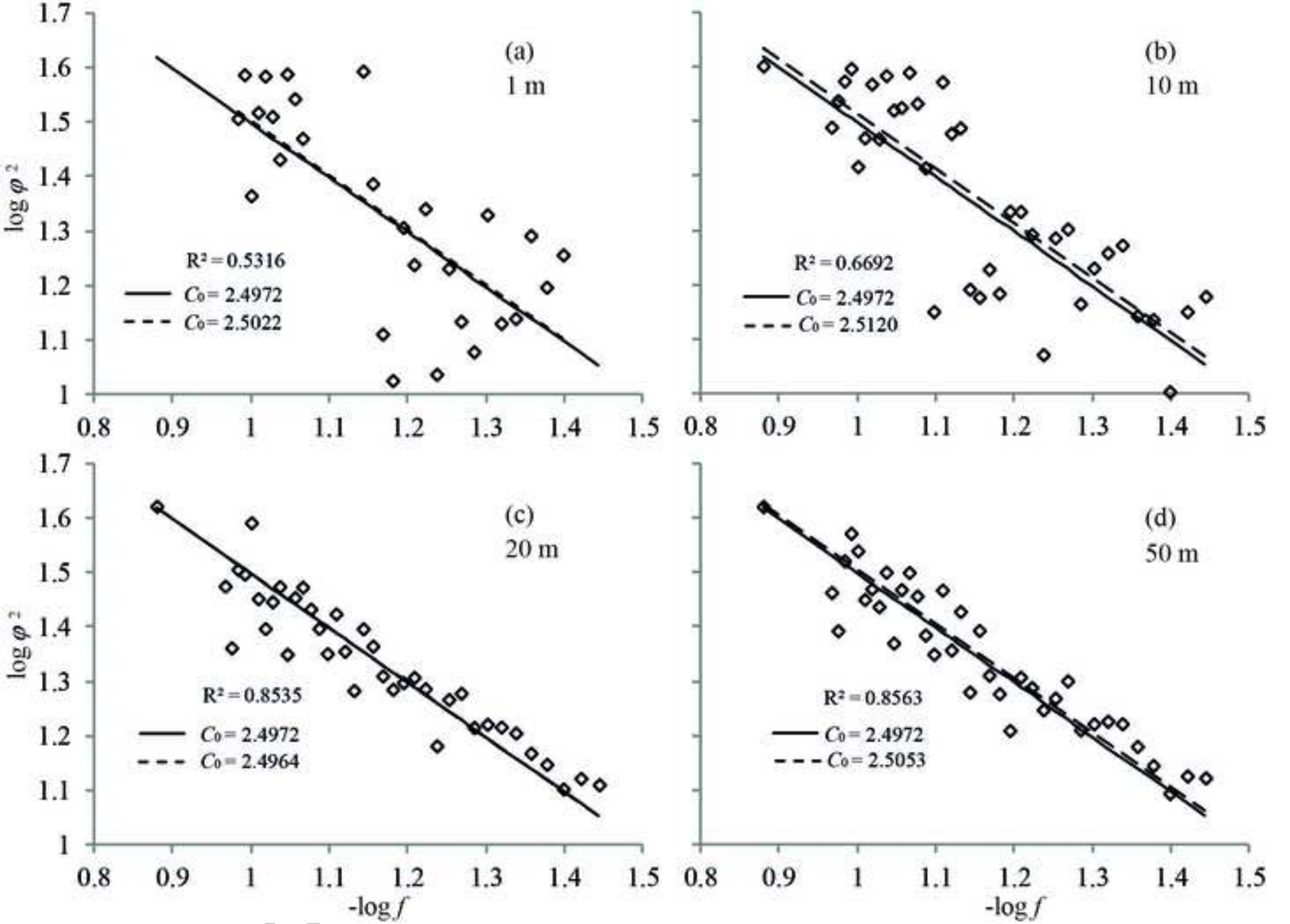
(a)
1 m
R² = 0.5316
C0 = 2.4972
C0 = 2.5022
(b)
10 m
R² = 0.6692
C0 = 2.4972
C0 = 2.5120
(c)
20 m
R² = 0.8535
C0 = 2.4972
C0 = 2.4964
(d)
50 m
R² = 0.8563
C0 = 2.4972
C0 = 2.5053
log φ²
-log f

Figure-6

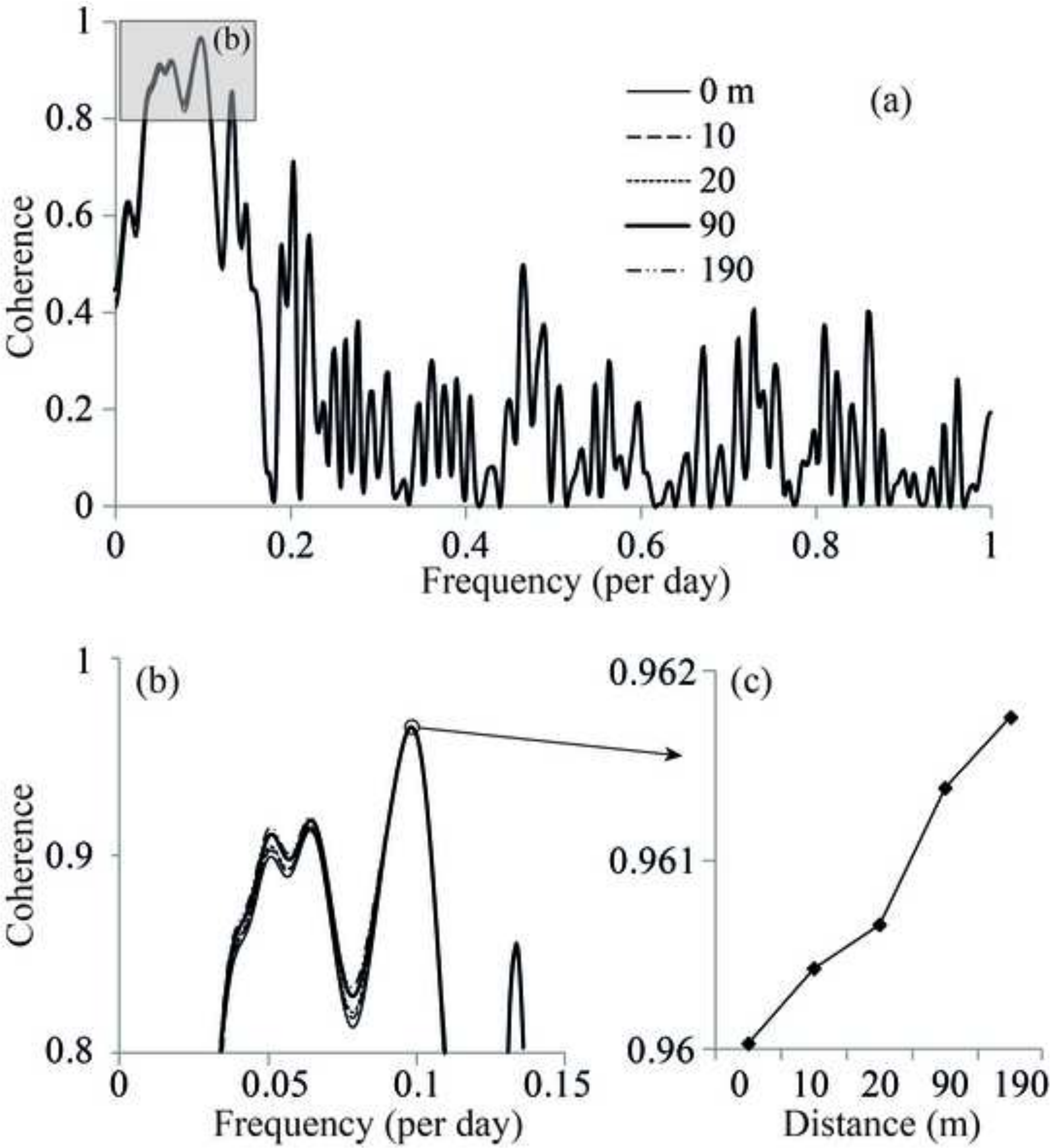

(b)
(a)
0 m
10
20
90
190
Coherence
Frequency (per day)
1
0.8
0.6
0.4
0.2
0
0.2
0.4
0.6
0.8
(b)
Coherence
1
0.9
0.8
0
0.05
0.1
0.15
Frequency (per day)
(c)
0.962
0.961
0.96
0
10
20
90
190
Distance (m)

Figure-7

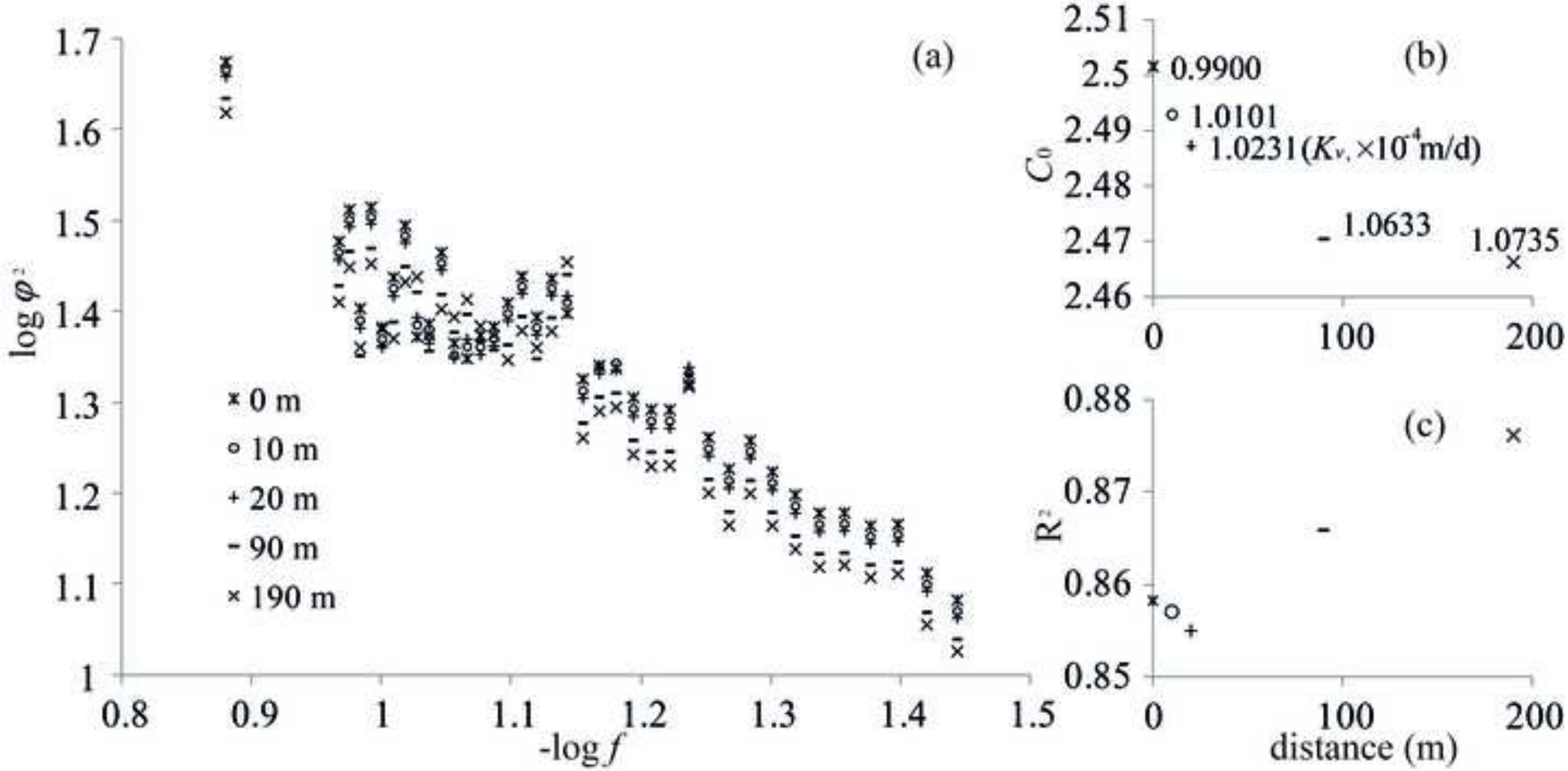
(a)
(b)
(c)
log φ²
-log f
0 m
10 m
20 m
90 m
190 m
C₀
0.9900
1.0101
1.0231 (Kv, ×10⁻⁴ m/d)
1.0633
1.0735
R²
distance (m)

Figure-8

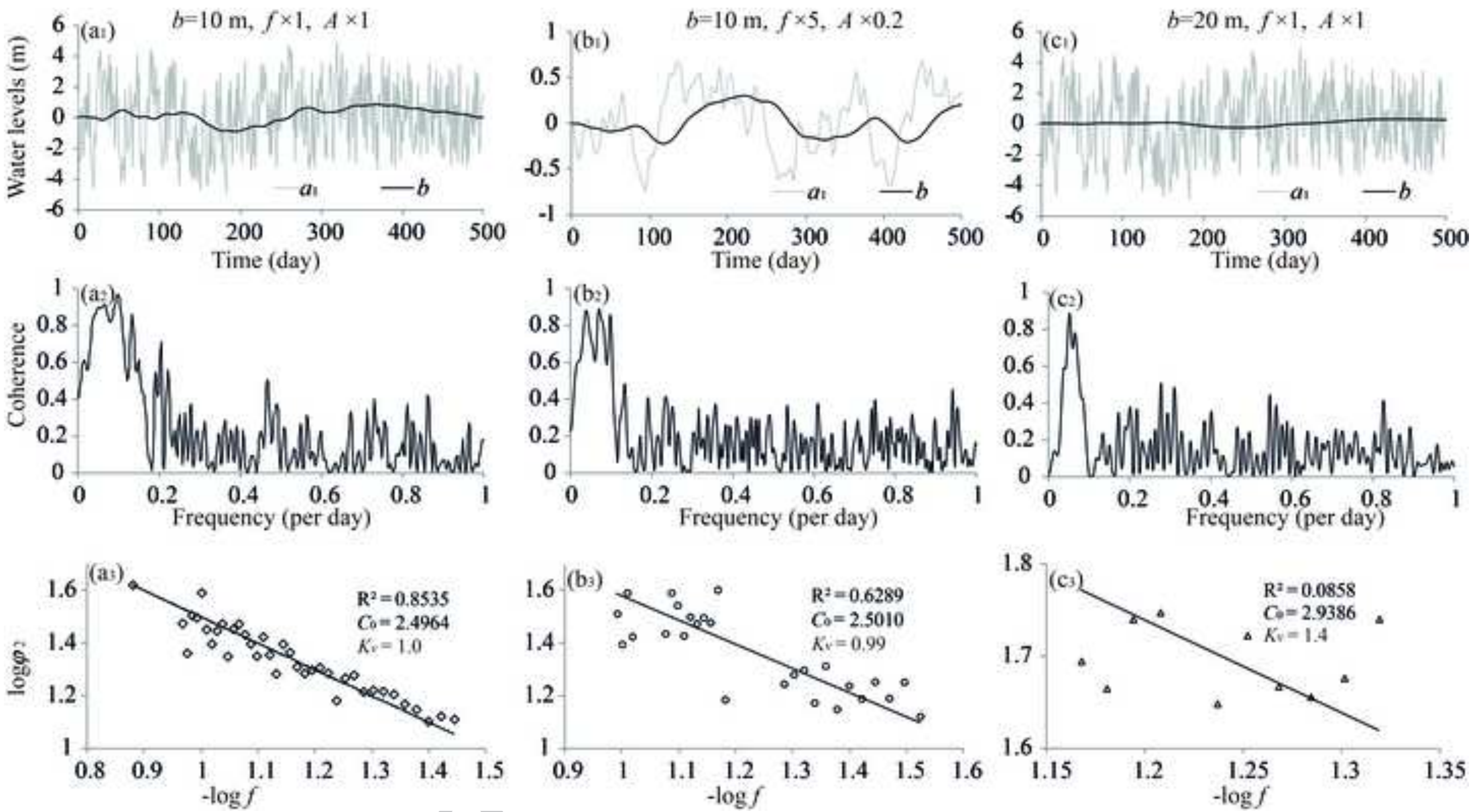

b=10 m, f ×1, A ×1
(a1)
Water levels (m)
a1
b
Time (day)
b=10 m, f ×5, A ×0.2
(b1)
b=20 m, f ×1, A ×1
(c1)
(a2)
Coherence
Frequency (per day)
(b2)
(c2)
(a3)
logφ2
R² = 0.8535
C0 = 2.4964
Kv = 1.0
-log f
(b3)
R² = 0.6289
C0 = 2.5010
Kv = 0.99
(c3)
R² = 0.0858
C0 = 2.9386
Kv = 1.4

Figure-9

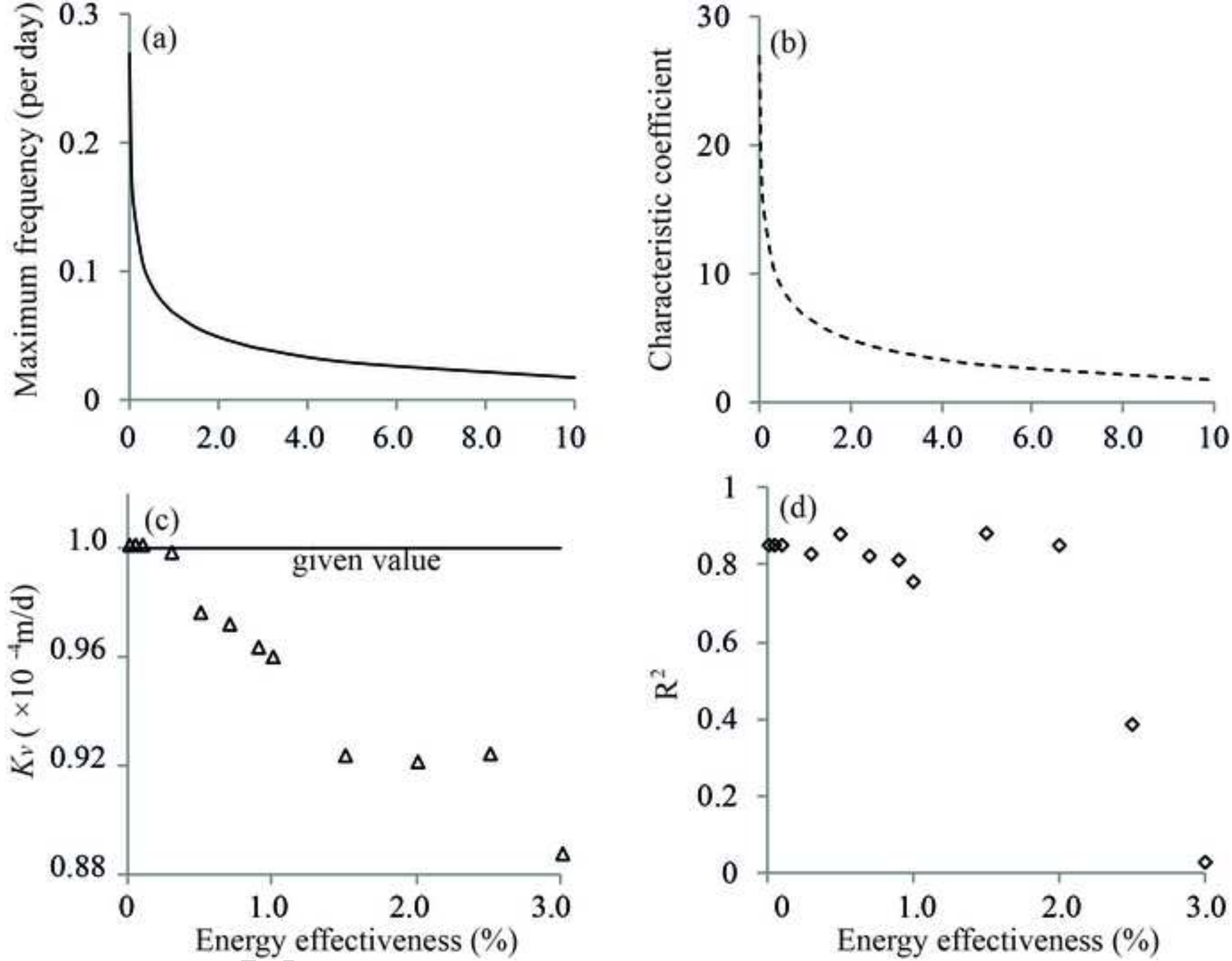

(a)
Maximum frequency (per day)
0.3
0.2
0.1
0
0
2.0
4.0
6.0
8.0
10
(b)
Characteristic coefficient
30
20
10
0
0
2.0
4.0
6.0
8.0
10
(c)
K_V (×10 $^{-4}$m/d)
1.0
0.96
0.92
0.88
given value
0
1.0
2.0
3.0
Energy effectiveness (%)
(d)
R^2
1
0.8
0.6
0.4
0.2
0
0
1.0
2.0
3.0
Energy effectiveness (%)

Figure-10

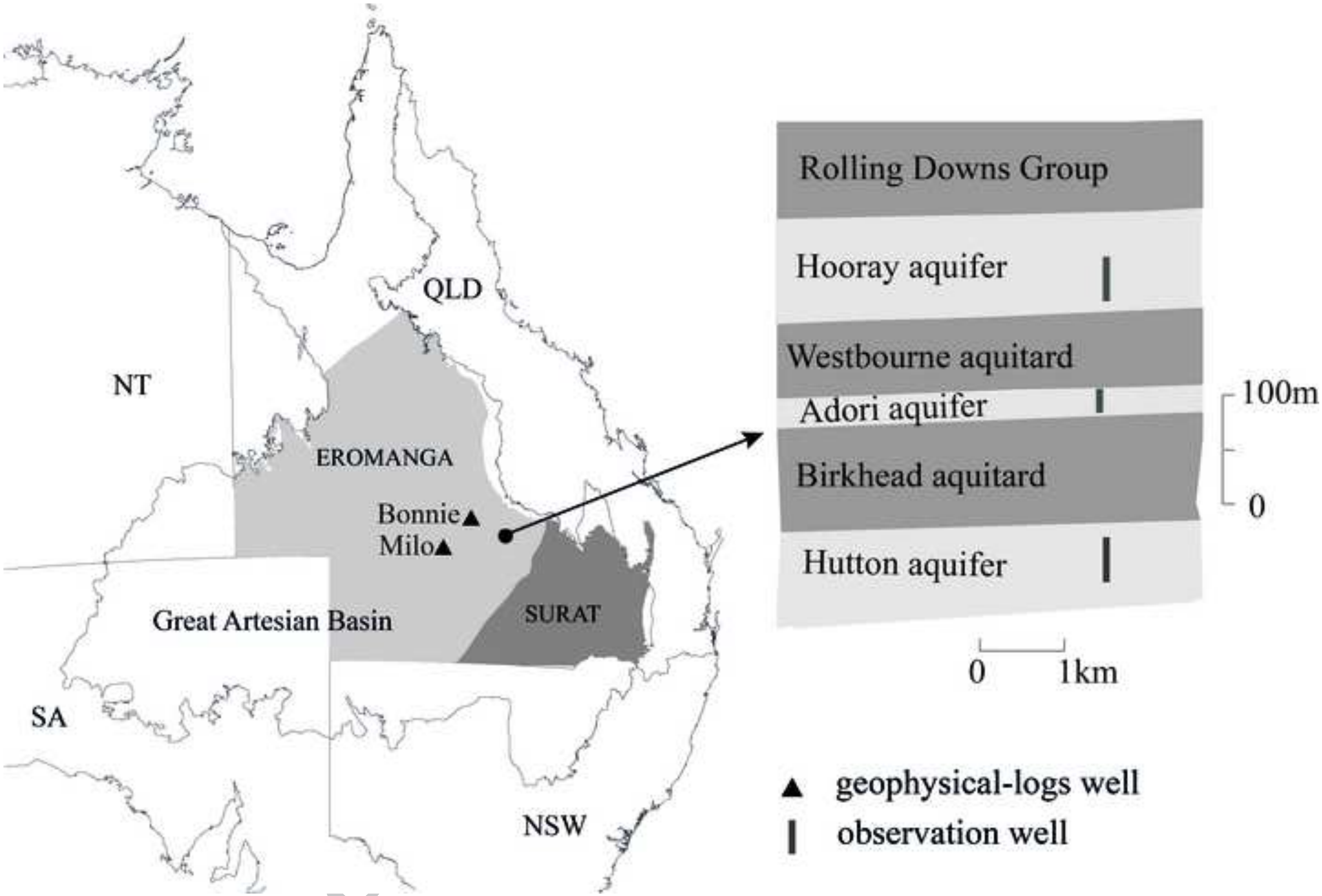

QLD
NT
EROMANGA
Bonnie
Milo
SURAT
Great Artesian Basin
SA
NSW
Rolling Downs Group
Hooray aquifer
Westbourne aquitard
Adori aquifer
Birkhead aquitard
Hutton aquifer
100m
0
0
1km
geophysical-logs well
observation well

Figure-11

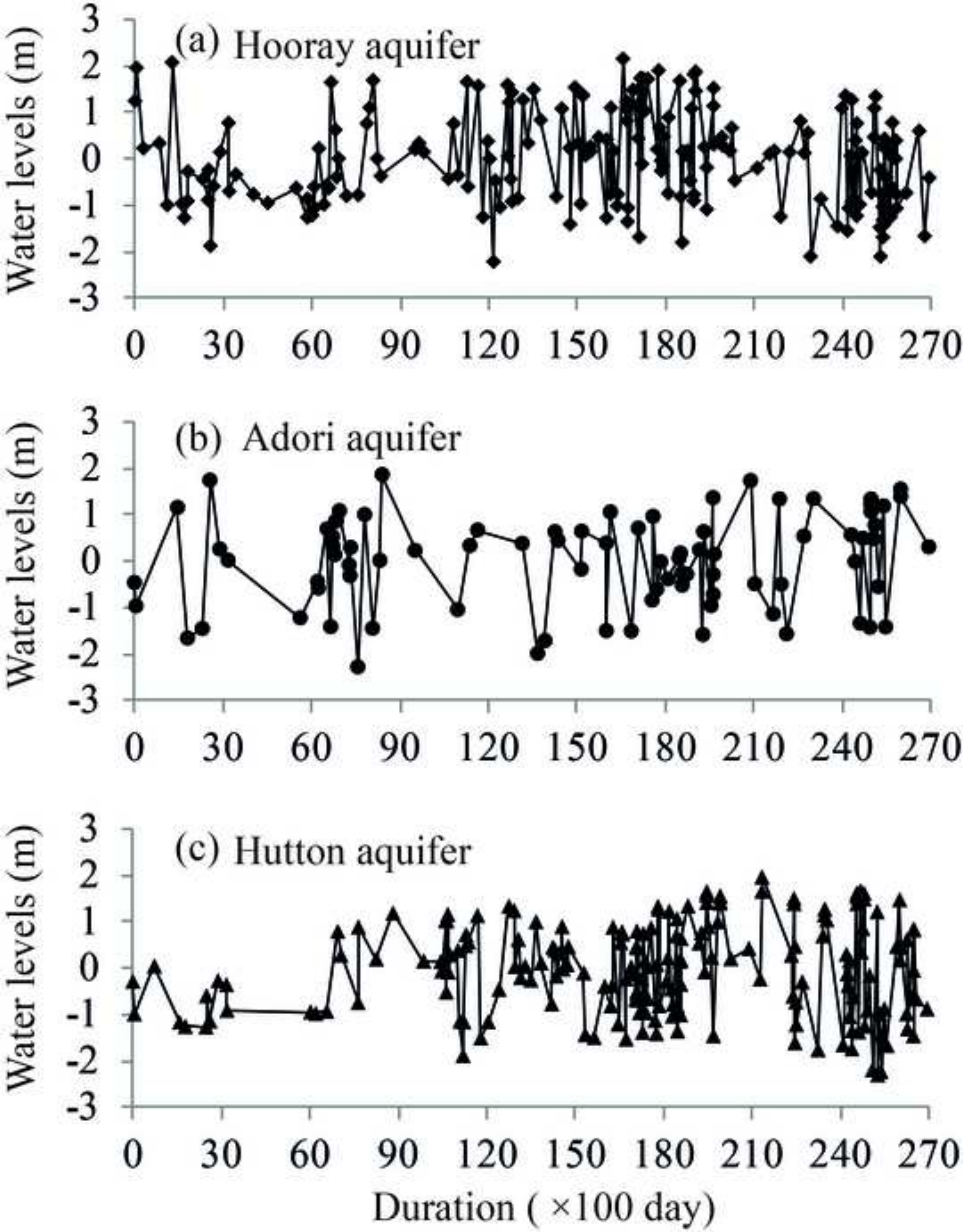
(a) Hooray aquifer
Water levels (m)
3
2
1
0
-1
-2
-3
0 30 60 90 120 150 180 210 240 270
(b) Adori aquifer
Water levels (m)
3
2
1
0
-1
-2
-3
0 30 60 90 120 150 180 210 240 270
(c) Hutton aquifer
Water levels (m)
3
2
1
0
-1
-2
-3
0 30 60 90 120 150 180 210 240 270
Duration (×100 day)

Figure-12

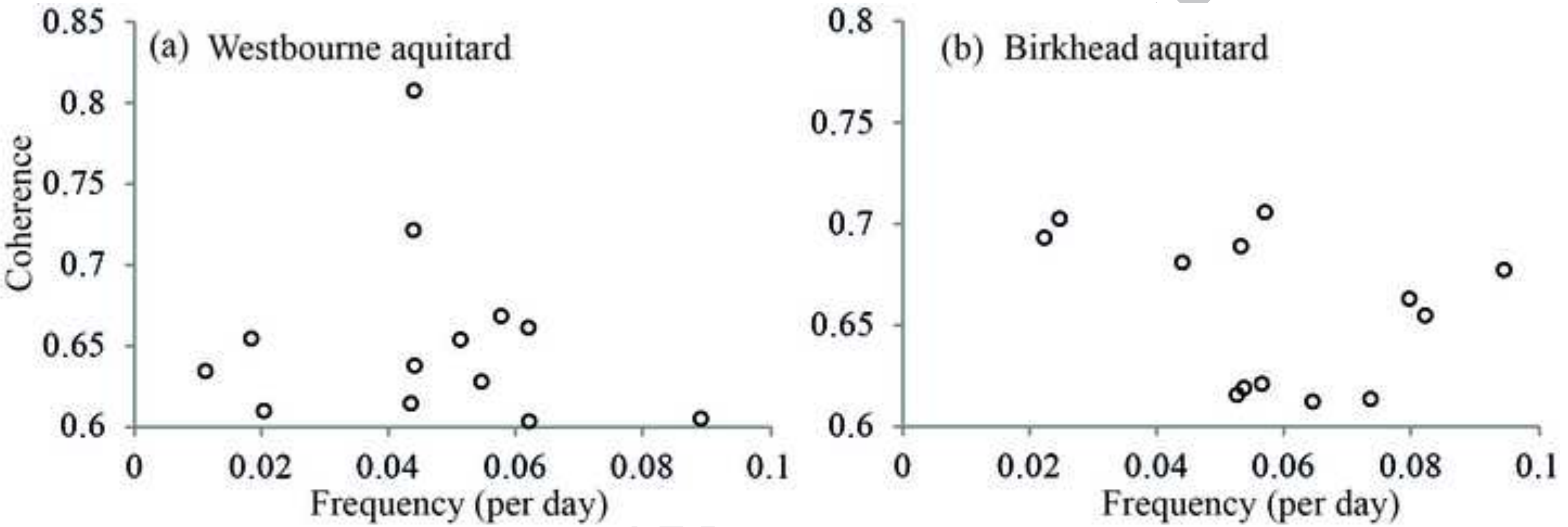
0.85
0.8
0.75
0.7
0.65
0.6
Coherence
(a) Westbourne aquitard
0
0.02
0.04
0.06
0.08
0.1
Frequency (per day)
0.8
0.75
0.7
0.65
0.6
(b) Birkhead aquitard
0
0.02
0.04
0.06
0.08
0.1
Frequency (per day)

Figure-13

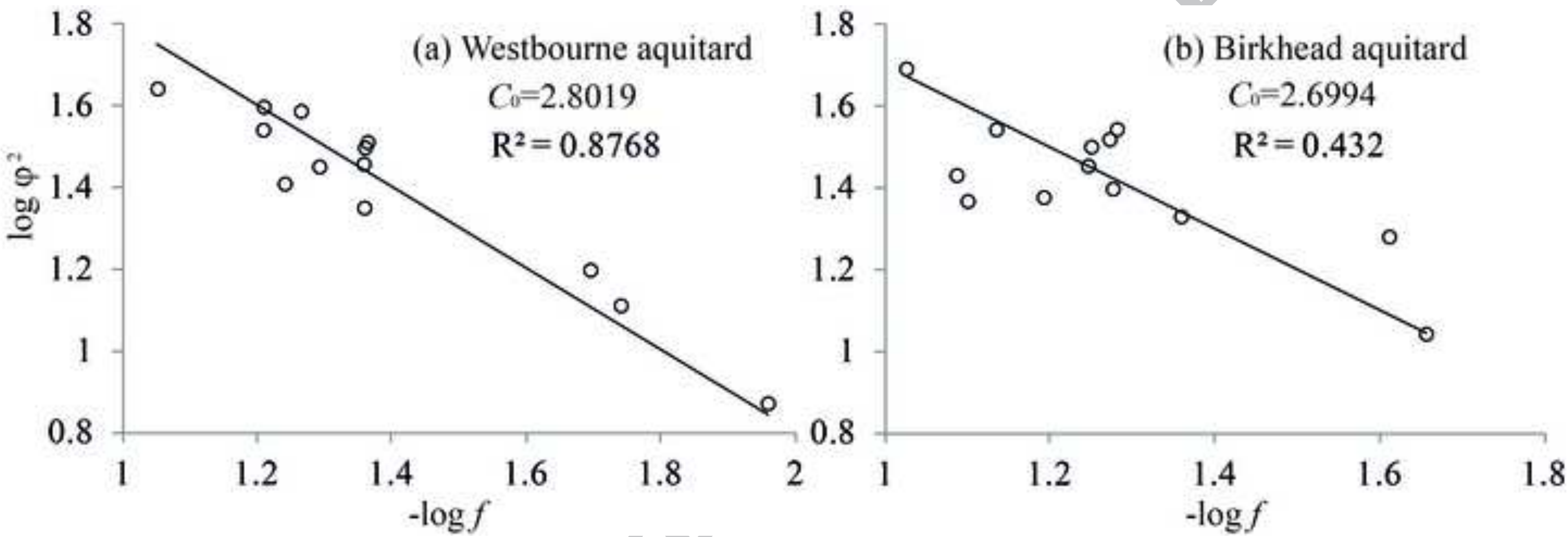

(a) Westbourne aquitard
C_0=2.8019
R^2 = 0.8768
log φ²
-log *f*
1.8
1.6
1.4
1.2
1
0.8
1
1.2
1.4
1.6
1.8
2
(b) Birkhead aquitard
C_0=2.6994
R^2 = 0.432
-log *f*
1.8
1.6
1.4
1.2
1
0.8
1
1.2
1.4
1.6
1.8

Table 1 Hydrogeological units in the Eastern Eromanga Basin

Formations	Lithology	*K* (m/d)	Thickness (m)	Hydrogeological unit
Rolling Downs Group	shale claystone siltstone	$< 10^{-5}$	400 (mean)	RDG aquitard
Cadna-Owie	sandstone	1.6-18.7	130 (mean)	Hooray aquifer
Hooray				
Westbourne	shale, siltstone, sandstone	unknown	87 (mean)	Westbourne aquitard
Adori	sandstone	10 (mean)	50 (mean)	Adori aquifer
Birkhead	shale, siltstone, sandstone	10^{-6} - 0.1	113 (mean)	Birkhead aquitard
Hutton	sandstone	0.1 -170	300 (mean)	Hutton aquifer
Evergreen	siltstone, sandstone, shale			
Precipice	sandstone			

K: the horizontal hydraulic conductivity in the aquifer and vertical hydraulic conductivity in the aquitard.

Research Highlights

1. We apply harmonic analysis approach in a multilayered leaky system;

2. We apply coherence analysis to identify leakage-induced water-level changes;

3. K_v of aquitard is calculated using water-level fluctuations in the aquifers;

4. Correlation between frequencies and phases support robust estimate of K_v.